Simulation of X-ray Absorption Spectroscopies with FDMNES

Yves Joly

Institut Néel, CNRS/Université Grenoble Alpes

1st CONEXS Summer School: "Analysing X-ray Spectroscopy"
Newcastle University, Newcastle, United Kingdom (September, 10-12, 2019)

References:

X-Ray Absorption and X-ray Emission Spectroscopy : Theory and Applications
Edited by J. A. van Bokhoven and C. Lamberti,
Wiley and sons (2016).
ISBN : 978-1-118-84423-6.

and more specifically, chapter 4 :
"*Theory of X-ray Absorption Near Edge Structure*"
Yves Joly and Stéphane Grenier.

About resonant diffraction:
"*Basics of Resonant Elastic X-ray Scattering theory*"
S. Grenier and Y. Joly,
J. Phys. : Conference Series **519**, 012001 (2014).

About X-ray Raman spectroscopy:
"Full potential simulation of x-ray Raman scattering spectroscopy"
Y. Joly, C. Cavallari, S. A. Guda, C. J. Sahle
J. Chem. Theory Comput. **13**, 2172-2177 (2017).

About Surface Resonant X-ray Diffraction:
"Simulation of Surface Resonant X-ray Diffraction"
Y. Joly, et al.
J. Chem. Theory Comput. DOI: 10.1021/acs.jctc.7b01032 (2017).

Soon→ International Tables for Crystallography, Volume I on XAS

Outline

I – Basics for mono-electronic simulations of X-ray absorption spectroscopies

II – Examples in XANES

III – X-ray Raman Scattering

IV – Resonant X-ray Diffraction

V – Presentation of the FDMNES software

Basics for mono-electronic simulations of X-ray absorption spectroscopies

A – From multi-electronic to mono-electronic

B – Transition matrices

C – Selection rules

D – Tensor approach

E - Final states calculation

A – From multi-electronic to mono-electronic

X-ray absorption spectroscopies are

- local spectroscopies
- Selective on the chemical specie
- Process involved are complex…

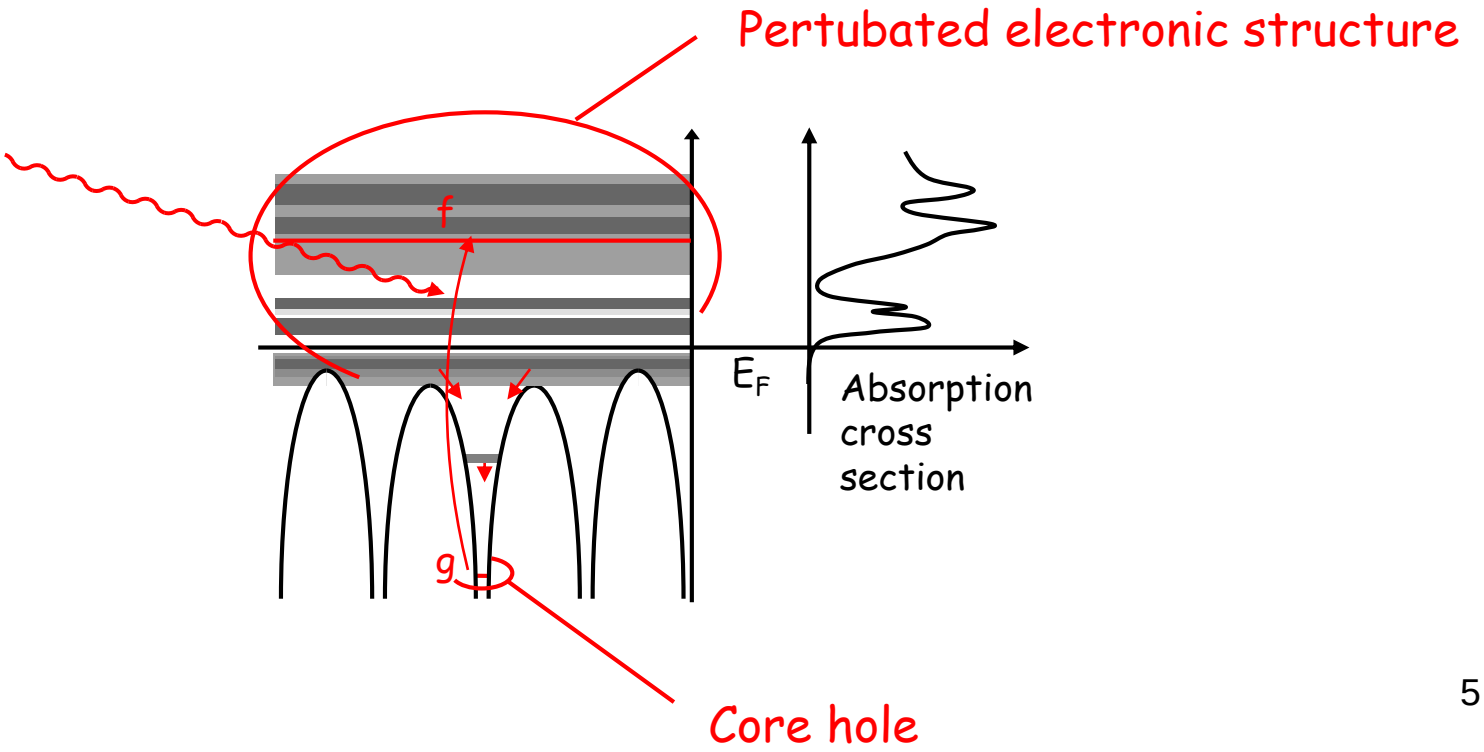

Characteristic times

1 – Time of the process « absorption of the photon »

$t_1 = 1/W_{fi}$, W_{fi} absorption probabilty

$t_1 < 10^{-20}$ s

2 – Time life of the core hole

$t_2 = \hbar / \Delta E_i$, ΔE_i width of the level

for 1s for Z = 20 up to 30, $\Delta E_i \approx 1$ eV

$t_2 \approx 10^{-15}$ à 10^{-16} s

3 – Relaxation time of the electron

Effect on all the electrons of the field created by the hole and the photoelectron. Many kinds of process, multielectronic.

$t_3 \approx 10^{-15}$ à 10^{-16} s

4 – Transit time of the photoelectron outward from the atom

Depends on the photoelectron kinetic energy, for E_c = 1 à 100 eV

$t_4 \approx 10^{-15}$ à 10^{-17} s

5 – Thermic vibration

$t_5 \approx 10^{-13}$ à 10^{-14} s

multi-electronic process can be seen at low energy of the photoelectron

X-ray absorption takes a snap shot of the pertubated material

Localized final states

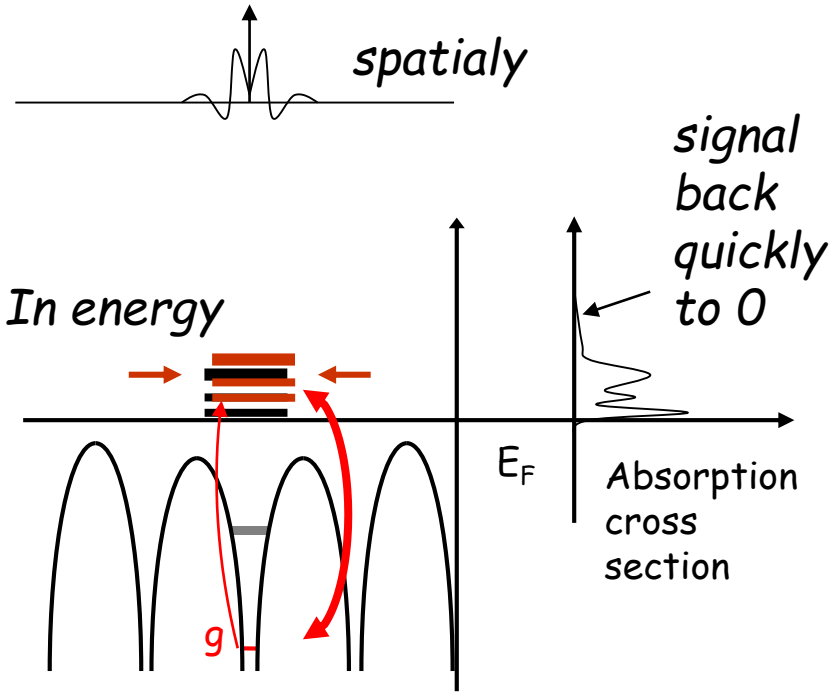

- Interaction with the hole
- Several possible electronic states…

Non localized final states

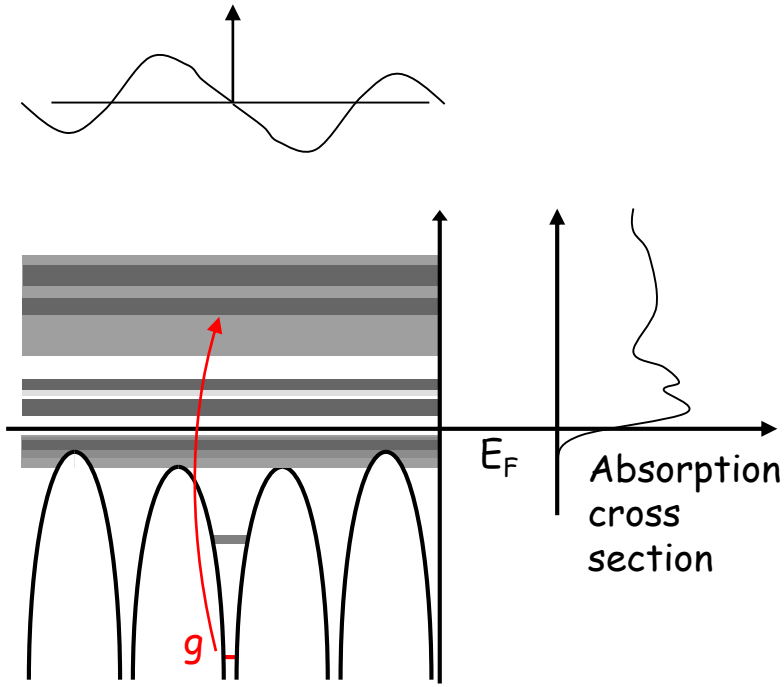

mono-electronic approach

Ground state theory: DFT

Localized final states

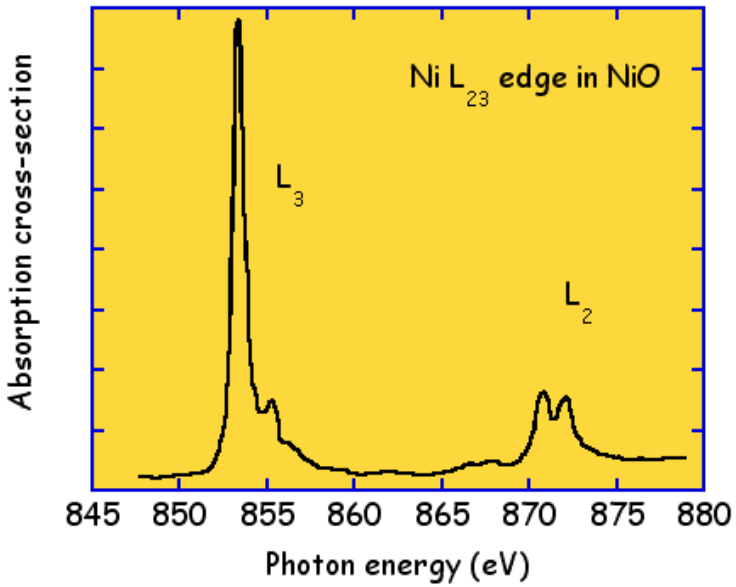

multiplet

A. Scherz, PhD Thesis, Berlin

Non localized final states

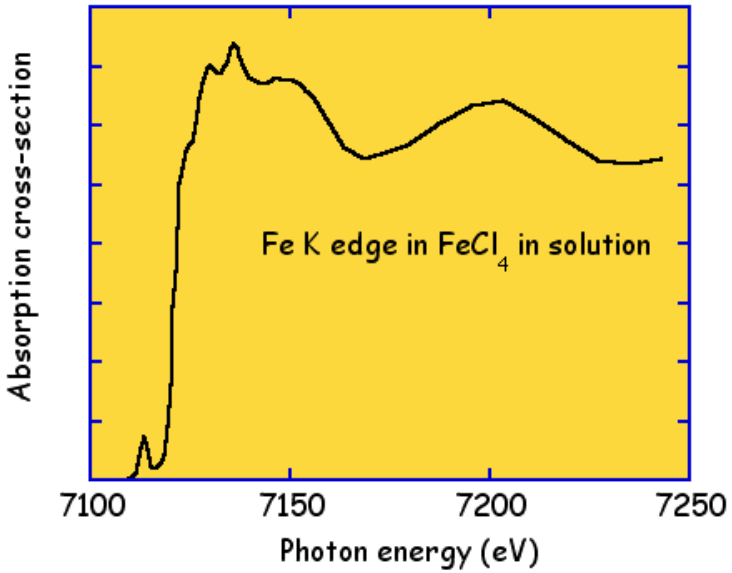

mono-electronic theory

O. Proux *et al.* FAME, ESRF

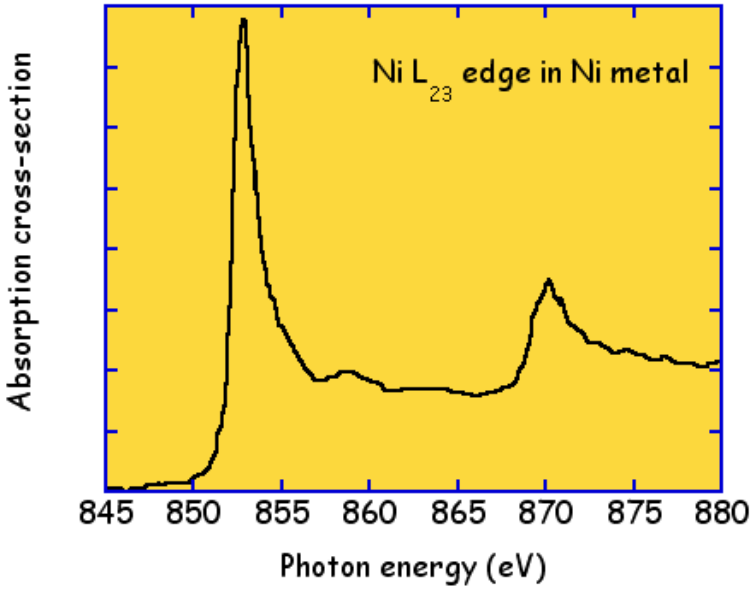

Intermediate situation …

Multiplet ligand field theory:

multi-electronic but mono-atomic

→ L_{23} edges of 3*d* elements

→ M_{45} edges of rare earth

DFT:

Multi-atomic but ground state theory (mono-electronic)

→ K, L_1 edges

→ L_{23} edges of heavy elements

Improvements in progress:

Bethe Salpeter Equation (Shirley…)

Time-Dependent DFT (Schwitalla…)

Multiplet ligand field theory using Wannier orbitals (Haverkort…)

Multichannel multiple scattering theory (Krüger and Natoli)

Dynamic mean field theory (Sipr…)

Quantum chemistry techniques, Configuration interaction…

Mono-electronic XANES formula

Multi-electronic system → Transition from I to F

F and I: multi-electronic final and initial states

Absorption cross section:

$$\sigma(\omega) = 4\pi^2\alpha\hbar\omega \sum_F |\langle F|o|I\rangle|^2 \delta(\hbar\omega - E_F + E_I) \qquad o = \boldsymbol{\varepsilon}\cdot\boldsymbol{r} + \frac{i}{2}\boldsymbol{\varepsilon}\cdot\boldsymbol{r}\boldsymbol{k}\cdot\boldsymbol{r}$$

Ground state (≈ mono-electronic) approximation:

$$\sigma(\omega) = 4\pi^2\alpha\hbar\omega S_0^2 \sum_{fg} |\langle f|o|g\rangle|^2 \delta(\hbar\omega - E_f + E_g + \Delta E_{scr})$$

Relaxation effect of the "other" electrons

f is by default calculated in an excited state:

- with a core-hole
- an extra electron on the first non occupied level

Core-hole and photoelectron time life effects

$$\sigma(\omega) = 4\pi^2\alpha\hbar\omega \sum_{fg} |\langle f|o|g\rangle|^2 \delta\left(\hbar\omega - E_f + E_g\right) \times \frac{1}{2\pi} \frac{\Gamma}{\left(E - E_f\right)^2 + \left(\frac{\Gamma}{2}\right)^2}$$

Lorentzian convolution

$$\Gamma = \Gamma_H + \Gamma_e(E)$$

Γ_H: core-hole width

Classical experiment: known tabulated values

M. O. Krause, J. H. Oliver, J. Phys. Chem. Ref. Data ***8****, 329 (1979)*

Experiment using High resolution fluorescence mode:
Reduced value

Γ_e: photoelectron state width

Due to all possible inelastic process
Increase with energy

B - Transition matrices

Plane wave :

$$\boldsymbol{A}(\boldsymbol{r},t) = A_0\left(ae^{i(\boldsymbol{k}.\boldsymbol{r}-\omega t)}\boldsymbol{\varepsilon} + a^{+}e^{-i(\boldsymbol{k}.\boldsymbol{r}-\omega t)}\boldsymbol{\varepsilon}^{*}\right)$$
$$\boldsymbol{E}(\boldsymbol{r},t) = i\omega A_0\left(ae^{i(\boldsymbol{k}.\boldsymbol{r}-\omega t)}\boldsymbol{\varepsilon} - a^{+}e^{-i(\boldsymbol{k}.\boldsymbol{r}-\omega t)}\boldsymbol{\varepsilon}^{*}\right)$$
$$\boldsymbol{B}(\boldsymbol{r},t) = iA_0\left(ae^{i(\boldsymbol{k}.\boldsymbol{r}-\omega t)}\boldsymbol{k}\times\boldsymbol{\varepsilon} - a^{+}e^{-i(\boldsymbol{k}.\boldsymbol{r}-\omega t)}\boldsymbol{k}\times\boldsymbol{\varepsilon}^{*}\right)$$

System Hamiltonian: $H = H_0 + H_I$

$$H_0 = mc^2 + \frac{\boldsymbol{p}^2}{2m} - eV + H_R$$

Interaction Hamiltonian:

$$H_I = \frac{e}{m}\left(\boldsymbol{p}.\boldsymbol{A} + \boldsymbol{S}.\boldsymbol{B} + \frac{i\omega}{2mc^2}\boldsymbol{S}.\boldsymbol{p}\times\boldsymbol{A}\right) + \frac{e^2}{2m}\boldsymbol{A}^2$$

relativistic spin-orbit interaction (not in Blum)

N. Bouldi *et al.* PRB **96**, 085123 (2017)

momentum

$$\boldsymbol{p} = -i\hbar\nabla$$

$$\boldsymbol{S} = \frac{\hbar}{2}\boldsymbol{\sigma}$$ ↖ Pauli Matrices

Transition between 2 states: $|\, i\rangle = |\, g; \boldsymbol{\varepsilon}_i, \boldsymbol{k}_i\rangle$ $|\, s\rangle = |\, f; \boldsymbol{\varepsilon}_s, \boldsymbol{k}_s\rangle$

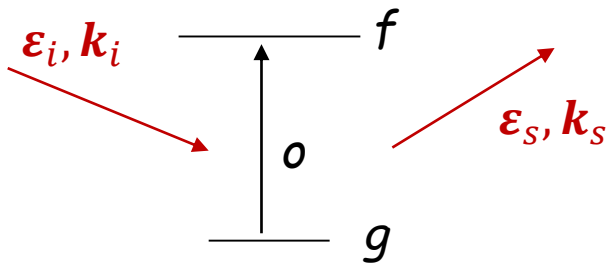

Transition operator: $T = H_I + H_I G(\mathcal{E}_i) H_I$ $G(\mathcal{E}_i) = \lim_{\eta \to 0^+} \dfrac{1}{\mathcal{E}_i - H + i\eta}$

$T \approx H_I + H_I G_0(\mathcal{E}_i) H_I$

At second order in (e/m): $T \approx T_1 + T_2$

$$T_1 = \frac{e}{m}\left(\boldsymbol{p}.\boldsymbol{A} + \boldsymbol{S}.\boldsymbol{B} + \frac{i\omega}{2mc^2}\boldsymbol{S}.\boldsymbol{p}\times\boldsymbol{A}\right)$$ Absorption & emission

$$T_2 = \left(\frac{e}{m}\right)^2 \left(\frac{m}{2}\boldsymbol{A}.\boldsymbol{A} + T_1 G_0(\mathcal{E}_i) T_1\right)$$ Scattering

Golden Rule : Dirac (1927) called by Fermi in 1950 Golden Rule n° 2

Absorption case

Transition probability (s^{-1}):

$$R_{fg} = \frac{2\pi}{\hbar} |\langle s|T_1|i\rangle|^2 \delta(E_f - E_g - \hbar\omega)$$

→ Cross section

$$\sigma_{fg} = \frac{2\pi h\alpha}{\omega m^2} \left|\langle f|\hat{O}|g\rangle\right|^2 \delta(E_f - E_g - \hbar\omega) \qquad \alpha = \frac{e^2}{2hc\varepsilon_0}$$

$$\hat{O} = \left(\boldsymbol{p}.\boldsymbol{\varepsilon} + i\tfrac{\hbar}{2}\boldsymbol{\sigma}.\boldsymbol{k}\times\boldsymbol{\varepsilon} + \frac{i\omega\hbar}{4mc^2}\boldsymbol{\sigma}.\boldsymbol{p}\times\boldsymbol{\varepsilon} \right) e^{i\boldsymbol{k}.\boldsymbol{r}}$$

$$\langle f|\hat{O}_E|g\rangle = \langle f|\boldsymbol{p}.\boldsymbol{\varepsilon}\left(1 + i\boldsymbol{k}.\boldsymbol{r} - \tfrac{1}{2}(\boldsymbol{k}.\boldsymbol{r})^2 + \cdots\right)|g\rangle$$

$$\langle f|\hat{O}_B|g\rangle = \langle f|i\tfrac{\hbar}{2}\boldsymbol{\sigma}.\boldsymbol{k}\times\boldsymbol{\varepsilon}\left(1 + i\boldsymbol{k}.\boldsymbol{r} - \tfrac{1}{2}(\boldsymbol{k}.\boldsymbol{r})^2 + \cdots\right)|g\rangle$$

$$\langle f|\hat{O}_E|g\rangle = \langle f|\boldsymbol{p}.\boldsymbol{\varepsilon}\left(1 + i\boldsymbol{k}.\boldsymbol{r} - \tfrac{1}{2}(\boldsymbol{k}.\boldsymbol{r})^2 + \cdots\right)|g\rangle$$

First term of the expansion:

Using: $\boldsymbol{p}.\boldsymbol{\varepsilon} = \dfrac{m}{i\hbar}[\boldsymbol{\varepsilon}.\boldsymbol{r}, H_0]$ $\qquad \langle f|[\boldsymbol{\varepsilon}.\boldsymbol{r}, H_0]\,|g\rangle = (E_g - E_f)\langle f|\boldsymbol{\varepsilon}.\boldsymbol{r}|g\rangle$

$$\langle f|\hat{O}_{E1}|g\rangle = i\frac{m}{\hbar}(E_g - E_f)\langle f|\boldsymbol{\varepsilon}.\boldsymbol{r}|g\rangle$$ Electric dipole (E1)

$$\langle f|\boldsymbol{\varepsilon}.\boldsymbol{r}|g\rangle = \iiint_{space} f(\boldsymbol{r})\boldsymbol{\varepsilon}.\boldsymbol{r}\,g(\boldsymbol{r})d\boldsymbol{r}$$

Second term of the expansion:

$$[zy, H_0] = [z, H_0]y + z[y, H_0] = i\frac{\hbar}{m}(p_z y + z p_y) = i\frac{\hbar}{m}(2p_z y + z p_y - p_z y)$$

$$= i\frac{\hbar}{m}(2p_z y - L_x) \qquad \Leftrightarrow \qquad p_z y = \frac{m}{2i\hbar}[zy, H_0] + \frac{1}{2}L_x$$

$$\boldsymbol{p}.\boldsymbol{\varepsilon}\boldsymbol{k}.\boldsymbol{r} = \frac{m}{2i\hbar}[\boldsymbol{\varepsilon}.\boldsymbol{r}\boldsymbol{k}.\boldsymbol{r}, H_0] + \frac{1}{2}\boldsymbol{k}\times\boldsymbol{\varepsilon}.\boldsymbol{L}$$ → Magnetic dipole

$$\langle f|\hat{O}_{E1}|g\rangle = i\frac{m}{\hbar}(E_g - E_f)\left\langle f\left|\frac{i}{2}\boldsymbol{\varepsilon}.\boldsymbol{r}\boldsymbol{k}.\boldsymbol{r}\right|g\right\rangle$$ Electric quadrupole (E2)

The formula

$$\sigma(\omega) = 4\pi^2 \alpha \hbar\omega \sum_{fg} |\langle f|o|g\rangle|^2 \delta\left(\hbar\omega - E_f + E_g\right)$$

light polarisation

light wave vector

Pauli matrices = $\frac{2}{\hbar} S$

$$o = \boldsymbol{\varepsilon}\cdot\boldsymbol{r}\left(1 + \tfrac{i}{2}\boldsymbol{k}\cdot\boldsymbol{r} - \tfrac{1}{6}(\boldsymbol{k}\cdot\boldsymbol{r})^2 \cdots\right) + \frac{1}{2mc}\left(\frac{\boldsymbol{k}}{k}\times\boldsymbol{\varepsilon}\right)\cdot(\boldsymbol{L} + \hbar\boldsymbol{\sigma}) + \frac{i\hbar\omega}{4mc^2}\boldsymbol{\sigma}\cdot(\boldsymbol{\varepsilon}\times\boldsymbol{r})$$

E1 | E2 | E3 | M1 | Spin position

El. dipole	El. quadrupole	El. octupole	Mag. Dipole	Dipole SP
$\Delta\ell = \pm 1$	$\Delta\ell = 0, \pm 2$	$\Delta\ell = \pm 1, \pm 3$	$\Delta\ell = 0$ $\Delta\sigma = 0, \pm 1$	$\Delta\ell = \pm 1$ $\Delta\sigma = 0, \pm 1$

N. Bouldi *et al.* PRB **96**, 085123 (2017)

C – Selection rules

Core states

K edge : $\ell = 0$ $\quad |\frac{1}{2}, -\frac{1}{2}\rangle = g_0(r)\begin{pmatrix} 0 \\ Y_0^0 \end{pmatrix}$ $\quad |\frac{1}{2}, \frac{1}{2}\rangle = g_0(r)\begin{pmatrix} Y_0^0 \\ 0 \end{pmatrix}$

L_{II} edge : $\ell = 1$ $\quad |\frac{1}{2}, -\frac{1}{2}\rangle = g_1(r)\begin{pmatrix} -\sqrt{\frac{2}{3}}Y_1^{-1} \\ \sqrt{\frac{1}{3}}Y_1^0 \end{pmatrix}$ $\quad |\frac{1}{2}, \frac{1}{2}\rangle = g_1(r)\begin{pmatrix} -\sqrt{\frac{1}{3}}Y_1^0 \\ \sqrt{\frac{2}{3}}Y_1^1 \end{pmatrix}$

Final states

Inside the absorbing atom (non magnetic case) :

$$f(\boldsymbol{r}) = \sum_{\ell m} a_{\ell m}^f(E) b_\ell(r) Y_\ell^m(\hat{r})$$

Spherical harmonic

Solution of the radial Schrödinger equation

Amplitudes. Contains the main dependence on the energy. Contains the information on the density of state

Transition operator

The expansion of $\boldsymbol{\varepsilon}\cdot\boldsymbol{r}$ and $\boldsymbol{k}\cdot\boldsymbol{r}$ in real spherical harmonics gives :

$$\boldsymbol{\varepsilon}\cdot\boldsymbol{r} = \sqrt{\frac{4\pi}{3}}\,\mathrm{r}Y_1^m$$

For example, polarization along z, wave vector along x :

$$\boldsymbol{\varepsilon}\cdot\boldsymbol{r} = z = r\cos\theta = c_{10}\mathrm{r}Y_1^0 \longrightarrow \ell_o = 1 \quad m_o = 0$$

$$\boldsymbol{\varepsilon}\cdot\boldsymbol{r}\,\boldsymbol{k}\cdot\boldsymbol{r} = kzx = kr^2\sin\theta\cos\theta\cos\varphi = c_{21}kr^2Y_2^1 \longrightarrow \ell_o = 2 \quad m_o = 1$$

The transition matrix is then:

$$\langle f|o|g\rangle = c_{\ell_o m_o}k^{\ell_o-1}\sum_{\ell m}a_{\ell m}^f(E)\left(\int_0^R b_\ell(r,E)\,g_{\ell_g}(r)r^{2+\ell_o}dr\right)\left(\iint Y_\ell^{m*}Y_{\ell_o}^{m_o}Y_{\ell_g}^{m_g}d\hat{r}\right)$$

Radial integral

Slowly varying with E

Strong dependence with ℓ_o

Gaunt coefficient

(tabulated constant related to the Clebch-Gordon coefficient)

non zero, only for some ℓ and m ⇨gives the selection rules

Angular integral non zero only for :

ℓ : same parity than $\ell_g + \ell_o$

$|\ell_g - \ell_o| \leq \ell \leq \ell_g + \ell_o$

Dipole: $\Delta\ell = \pm 1$

Quadrupole : $\Delta\ell = 0, \pm 2$

	Dipole probed state	Quadrupole probed state
K, L_I, M_I, N_I, O_I	p	s - d
$L_{II}, L_{III}, M_{II}, M_{III}, N_{II}, N_{III}, O_{II}, O_{III}$	s - d	p - f
$M_{IV}, M_V, N_{IV}, N_V, O_{IV}, O_V$	p - f	s - d - g

with complex spherical harmonics :

$m = m_o + m_g$

K edge case :

dipole component and polarization along z :

one probes the p_z states projected onto the absorbing atom

quadrupole component, polarization along z, wave vector along x :

one probes the d_{xz} states projected onto the absorbing atom

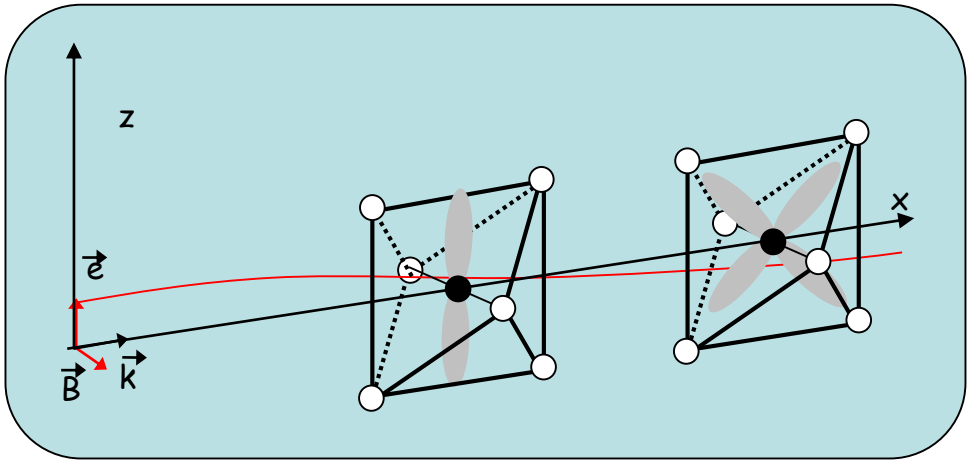

XANES is very sensitive to the 3D environment

$$\sigma(\omega) = 4\pi^2\alpha\hbar\omega \sum_{fg} |\langle f|o|g\rangle|^2 \delta(\hbar\omega - E_f + E_g)$$

$$\rho(E_f) = \sum_f \langle f|f\rangle = \sum_{\ell m} \int 4\pi r^2 b_\ell^2 dr \sum_f \left|a_{\ell m}^f\right|^2$$

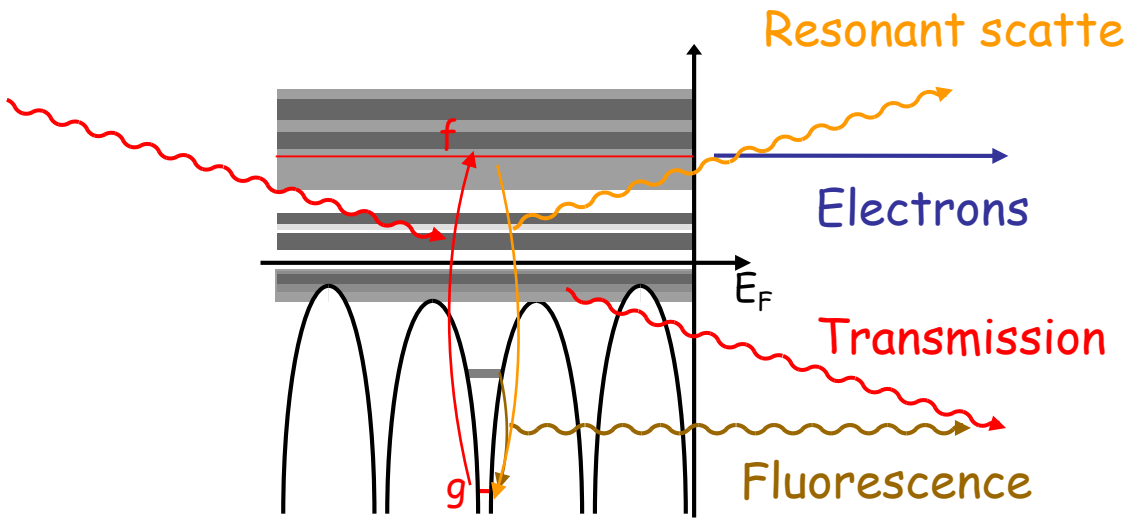

Whatever is the detection mode,

- one measures the transition probability between an initial state g and a final state f

- Thus one measures the state density at all energy

- The state density depends on the electronic and geometric surrounding of the absorbing atom

D- Tensor approach and multipole analysis

Dipole Quadrupole

$$\langle f|o|g\rangle = D + i\frac{k}{2}Q + \cdots \qquad o = \boldsymbol{\varepsilon}\cdot\boldsymbol{r} + \frac{i}{2}\boldsymbol{\varepsilon}\cdot\boldsymbol{r}\boldsymbol{k}\cdot\boldsymbol{r} + \cdots$$

Signal amplitude :

$$\langle g|o_s^*|f\rangle\langle f|o_i|g\rangle = D_s^* D_i + i\frac{k}{2}(D_s^* Q_i - Q_s^* D_i) + \frac{k^2}{4}Q_s^* Q_i \ldots$$

Dipole-Dipole — rank 2 tensor

Dipole-Quadrupole — rank 3 tensor

Quadrupole Quadrupole — rank 4 tensor

$$D_{\alpha\beta} = \sum_{fg}\langle g|\alpha|f\rangle\langle f|\beta|g\rangle \qquad \alpha = x, y \text{ or } z$$

$$A = \sum_{\alpha\beta}\varepsilon_\alpha^{s*}\varepsilon_\beta^{i}D_{\alpha\beta} + \frac{ik}{2}\sum_{\alpha\beta\gamma}\varepsilon_\alpha^{s*}\varepsilon_\beta^{i}\left(u_\gamma^{i}I_{\alpha\beta\gamma} - u_\gamma^{s}I_{\beta\alpha\gamma}^{*}\right) + \frac{k^2}{4}\sum_{\alpha\beta\gamma\delta}\varepsilon_\alpha^{s*}\varepsilon_\beta^{i}u_\gamma^{s}u_\delta^{i}Q_{\alpha\gamma\beta\delta}$$

$$A_{dd} = \begin{bmatrix}\varepsilon_x^{s*} & \varepsilon_y^{s*} & \varepsilon_z^{s*}\end{bmatrix}\begin{bmatrix}D_{xx} & D_{xy} & D_{xz}\\ D_{yx} & D_{yy} & D_{yz}\\ D_{zx} & D_{zy} & D_{zz}\end{bmatrix}\begin{bmatrix}\varepsilon_x^{i}\\ \varepsilon_y^{i}\\ \varepsilon_z^{i}\end{bmatrix}$$

9 components

$D_{\alpha\beta} = D_{\beta\alpha}^*$: complex when magnetic material

$D_{\alpha\alpha}$: real

Cartesian tensor

$$A = \sum_{\alpha\beta} \varepsilon_\alpha^{s*} \varepsilon_\beta^{i} D_{\alpha\beta} + \frac{ik}{2} \sum_{\alpha\beta\gamma} \varepsilon_\alpha^{s*} \varepsilon_\beta^{i} \left(u_\gamma^{i} I_{\alpha\beta\gamma} - u_\gamma^{s} I^{*}_{\beta\alpha\gamma} \right) + \frac{k^2}{4} \sum_{\alpha\beta\gamma\delta} \varepsilon_\alpha^{s*} \varepsilon_\beta^{i} u_\gamma^{s} u_\delta^{i} Q_{\alpha\gamma\beta\delta}$$

Spherical tensor

$$A = \sum_{\substack{\ell=0,2 \\ m=-\ell,\ell}} (-1)^{\ell+m} T_\ell^m D_\ell^m + i \sum_{\substack{\ell=1,3 \\ m=-\ell,\ell}} (-1)^{\ell+m} U_\ell^m I_\ell^m + \sum_{\substack{\ell=0,4 \\ m=-\ell,\ell}} (-1)^{\ell+m} V_\ell^m Q_\ell^m$$

$$D_0^0 = \frac{1}{\sqrt{3}} \left(D_{xx} + D_{yy} + D_{zz} \right)$$

$$D_1^0 = -\frac{i}{\sqrt{2}} \left(D_{xy} - D_{yx} \right) = \ell_z$$

$$D_2^0 = \frac{1}{\sqrt{6}} \left(2D_{zz} - D_{xx} - D_{yy} \right)$$

$$T_0^0 = \frac{1}{\sqrt{3}} \left(\varepsilon_x^{s*} \varepsilon_x^{i} + \varepsilon_y^{s*} \varepsilon_y^{i} + \varepsilon_z^{s*} \varepsilon_z^{i} \right) = \frac{1}{\sqrt{3}} \vec{\varepsilon}_s . \vec{\varepsilon}_i$$

$$T_1^0 = -\frac{i}{\sqrt{2}} \left(\varepsilon_x^{f*} \varepsilon_y^{i} - \varepsilon_y^{f*} \varepsilon_x^{i} \right) = -\frac{i}{\sqrt{2}} \left(\vec{\varepsilon}_s^{\,*} \times \vec{\varepsilon}_i \right)_z$$

E1-E1 part :

$$A_{dd} = \frac{1}{3} \left(\vec{\varepsilon}_s^{\,*} . \vec{\varepsilon}_i \right) Tr(D) - \frac{i}{\sqrt{2}} \left(\vec{\varepsilon}_s^{\,*} \times \vec{\varepsilon}_i \right) . \vec{\ell} + \sum_{m=-2,2} T_2^m D_2^m$$

Electric monopole (isotrope)

Magnetic dipole

Electric quadrupole

Cubic symmetry

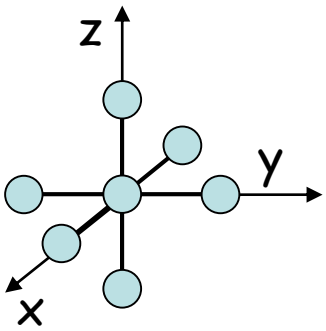

$$\begin{bmatrix} D_{zz} & 0 & 0 \\ 0 & D_{zz} & 0 \\ 0 & 0 & D_{zz} \end{bmatrix}$$

$$A_{dd} = \left(\vec{\varepsilon}_s^{\,*}.\vec{\varepsilon}_i\right) D_{zz}$$ Electric monopole

$$\longrightarrow \quad A_{dd} = D_{zz}$$

4/mmm

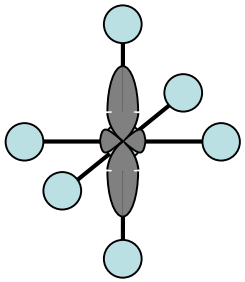

$$\begin{bmatrix} D_{xx} & 0 & 0 \\ 0 & D_{xx} & 0 \\ 0 & 0 & D_{zz} \end{bmatrix}$$

$$A_{dd} = \tfrac{1}{3}\left(\vec{\varepsilon}_s^{\,*}.\vec{\varepsilon}_i\right)(D_{zz} + 2D_{xx}) + \tfrac{1}{3}(D_{zz} - D_{xx})\left(2\varepsilon_z^{s*}\varepsilon_z^{i} - \varepsilon_x^{s*}\varepsilon_x^{i} - \varepsilon_y^{s*}\varepsilon_y^{i}\right)$$

Electric quadrupole

$$\vec{\varepsilon}_i = \vec{\varepsilon}_s = \begin{pmatrix} \sin\theta\cos\varphi \\ \sin\theta\sin\varphi \\ \cos\theta \end{pmatrix} \longrightarrow$$

$$\sqrt{\tfrac{16\pi}{5}}\,Y_2^0(\theta,\varphi)$$

$$A_{dd} = \tfrac{1}{3}(D_{zz} + 2D_{xx}) + \tfrac{1}{3}(D_{zz} - D_{xx})\left(3\cos^2\theta - 1\right)$$

4/m'm'm

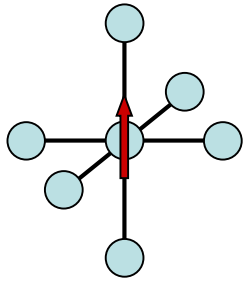

$$\begin{bmatrix} D_{xx} & iD_{xy}^{i} & 0 \\ -iD_{xy}^{i} & D_{xx} & 0 \\ 0 & 0 & D_{zz} \end{bmatrix}$$

$$A_{dd} = \tfrac{1}{3}\left(\vec{\varepsilon}_s^{\,*}.\vec{\varepsilon}_i\right)\mathrm{Tr}(D) - \tfrac{i}{\sqrt{2}}\left(\vec{\varepsilon}_s^{\,*} \times \vec{\varepsilon}_i\right).\vec{\ell} + T_2^0 D_2^0$$

Magnetic dipole

$$\vec{\varepsilon}_i = \vec{\varepsilon}_s = \tfrac{1}{\sqrt{2}}\begin{pmatrix} 1 \\ \pm i \\ 0 \end{pmatrix} \longrightarrow \pm D_{xy}^{i} = \pm \ell_z$$

$$\sum_{\substack{\ell=0,2\\ m=-\ell,\ell}} (-1)^{\ell+m} T_\ell^m D_\ell^m + i \sum_{\substack{\ell=1,3\\ m=-\ell,\ell}} (-1)^{\ell+m} T_\ell^m I_\ell^m + \sum_{\substack{\ell=0,4\\ m=-\ell,\ell}} (-1)^{\ell+m} T_\ell^m Q_\ell^m$$

ℓ		dipole-dipole E1-E1	dipole-quadrupole E1-E2		quadrupole-quadrup. E2-E2
0	monopole	charge ρ_p ++			charge ρ_d ++
1	dipole	moment m_p -+	n +-	toroidal -- moment t	Connected to moment m_d -+
2	quadrupole	++	toroidal axis (t,m) +-	(n,m) --	++
3	octupole		(n,m,m) +-	(t,m,m) --	-+
4	hexadecapole				++

electric
magnetic

Sign under time reversal, inversion : ++, +-, -+, --

One can get E1-E1, E1-E2, E2-E2 terms

But in principal also …
M1-M1, E1-M1 ….

E- Final state calculation

About the potential

As in most electronic structure calculations the choice of the potential is important

One body calculation = local density approximation (LSDA)

Potential = Coulomb potential + exchange-correlation potential

Depends just on the electron density

Different theories

- Xα
- Hedin and Lundqvist
- Perdew.....

Depends also on the electron kinetic energy

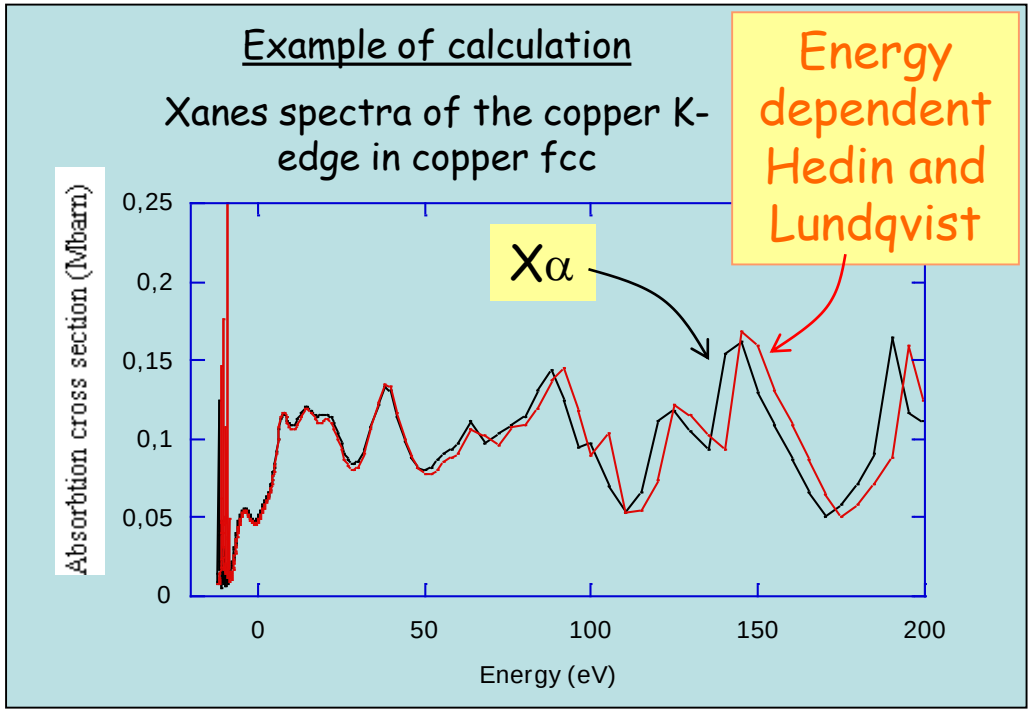

And about the shape of the potential

The muffin-tin approximation ⟶ the MT of the LMTO program

(almost) always used in the multiple scattering theory

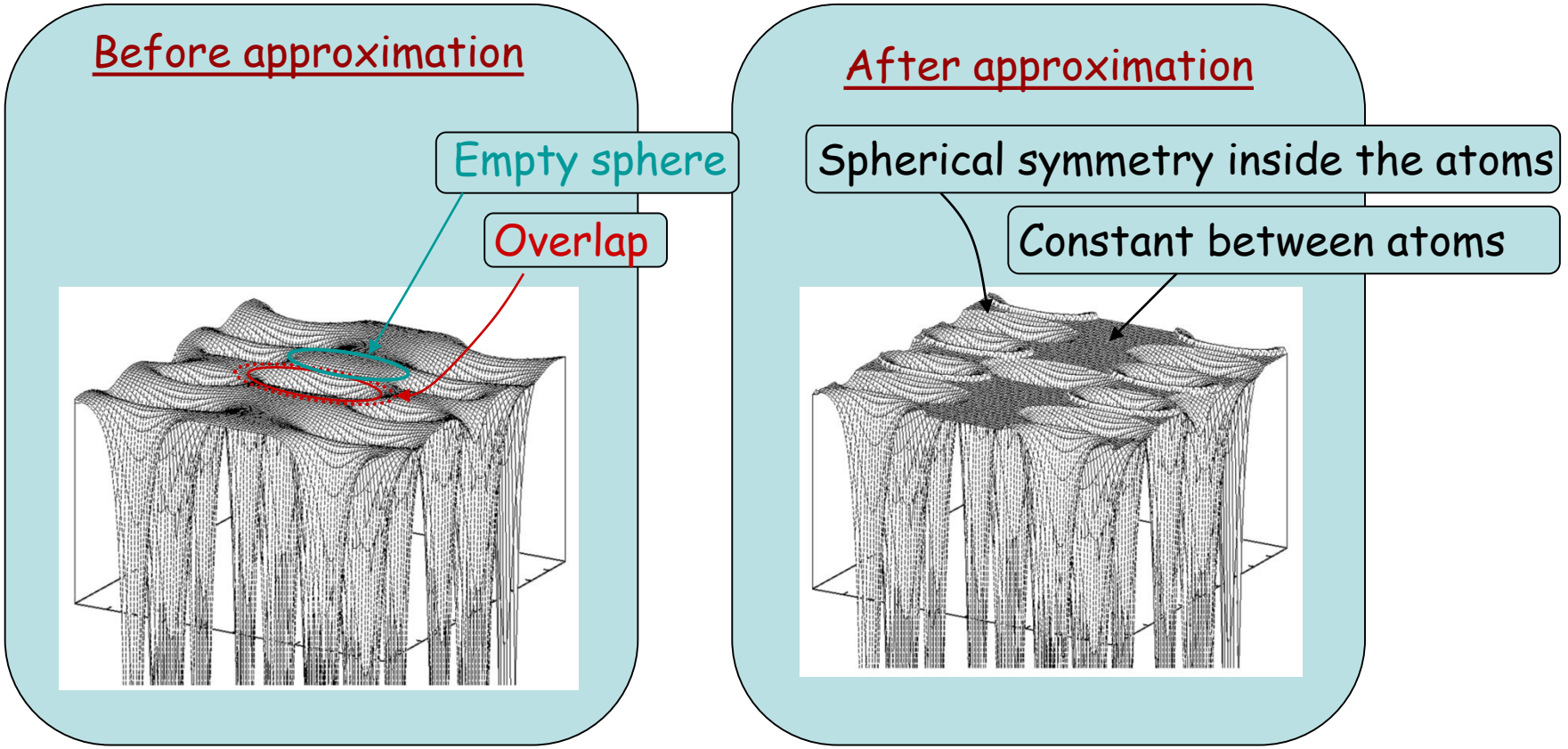

With the muffin-tin, there are always 2 parameters : overlap and interstitial constant

The multiple scattering theory

Two ways to explain it :

the Green function approach

the scattering wave approach

Just one atom :

We build a complete basis in the surrounding vacuum (Bessel and Hankel functions)

We look how the atom scatters all the Bessel functions (phase shift theory)

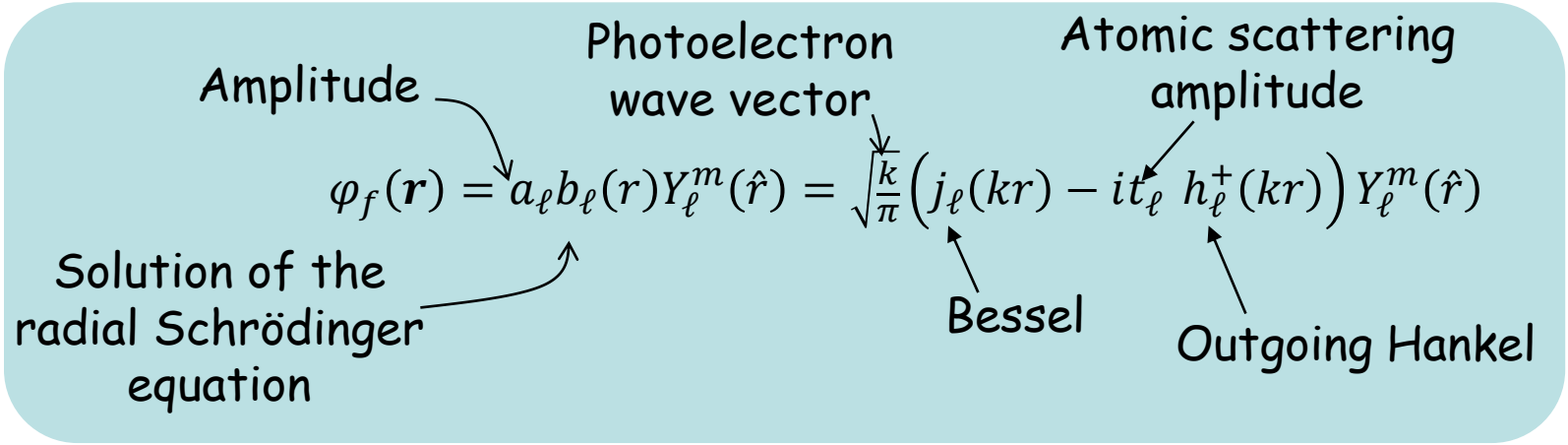

Several atoms (cluster)

Each atom receives not only the central Bessel function but also all the back scattered waves from all the other atoms

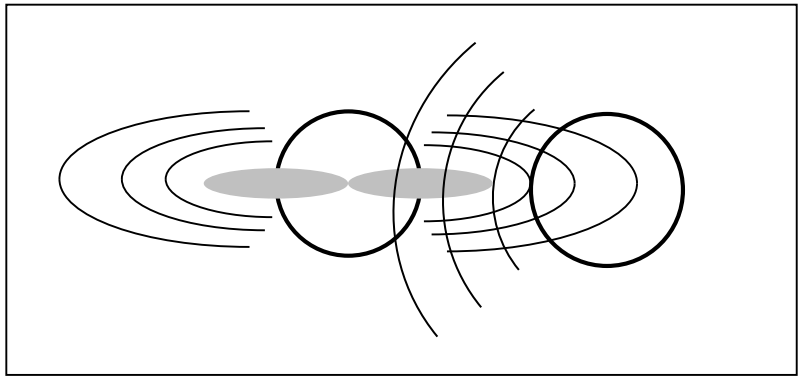

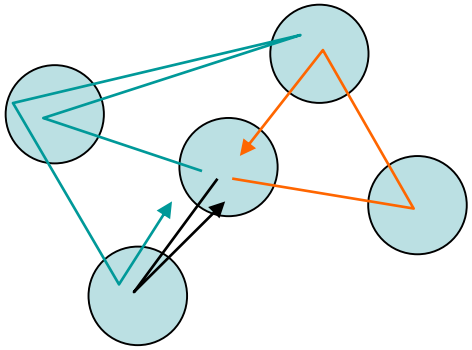

The problem is not anymore spherical

We have to fill a big matrix with the scattering atomic amplitudes of each atom and the propagation function from one atom to another

Matrix containing the atomic scattering amplitudes

Matrix containing the geometrical terms corresponding to the scattering from any site "a" of the harmonic L=(ℓ,m) towards any site "b" with the harmonic L'

$$\tau_{LL'}^{aa} = \left[\frac{1}{1-TH}T\right]_{LL'}^{aa}$$

Then one gets the scattering amplitude of the central atom in the presence of its neighboring atoms.

When no spin-orbit:

Wave function in the atom: $$\varphi_f(\boldsymbol{r}) = \sum_{\ell m} a^f_{\ell m}(E_f) b_\ell(r, E_f) Y^m_\ell(\hat{r}) \chi_{\sigma_f}$$

From the optical theorem : $$\sum_f a^f_{\ell m} a^{f*}_{\ell' m'} = -\mathcal{I}\left(\tau^{\ell' m'}_{\ell m}\right)$$

one gets for the absorption cross section:

$$\sigma(\omega) = -4\pi^2 \alpha \hbar \omega \sum_g \sum_{\ell m \ell' m'} \mathcal{I}\left(\langle g|o^*|b_\ell Y^m_\ell\rangle \tau^{\ell' m'}_{\ell m} \left\langle b_{\ell'} Y^{m'}_{\ell'} \middle| o \middle| g \right\rangle\right)$$

Multiple scattering amplitude

Green's function

The finite difference method

Discretization of the Schrödinger equation on a grid of points

$$\frac{\partial^2 \varphi_f(x)}{\partial x^2} = \frac{\varphi_f(x+h) + \varphi_f(x-h) - 2\varphi_f(x)}{h^2}$$

$$\left(\frac{6}{h^2} + V_i - E\right)\varphi_{f,i} - \sum_j \frac{1}{h^2}\varphi_{f,j} = 0$$

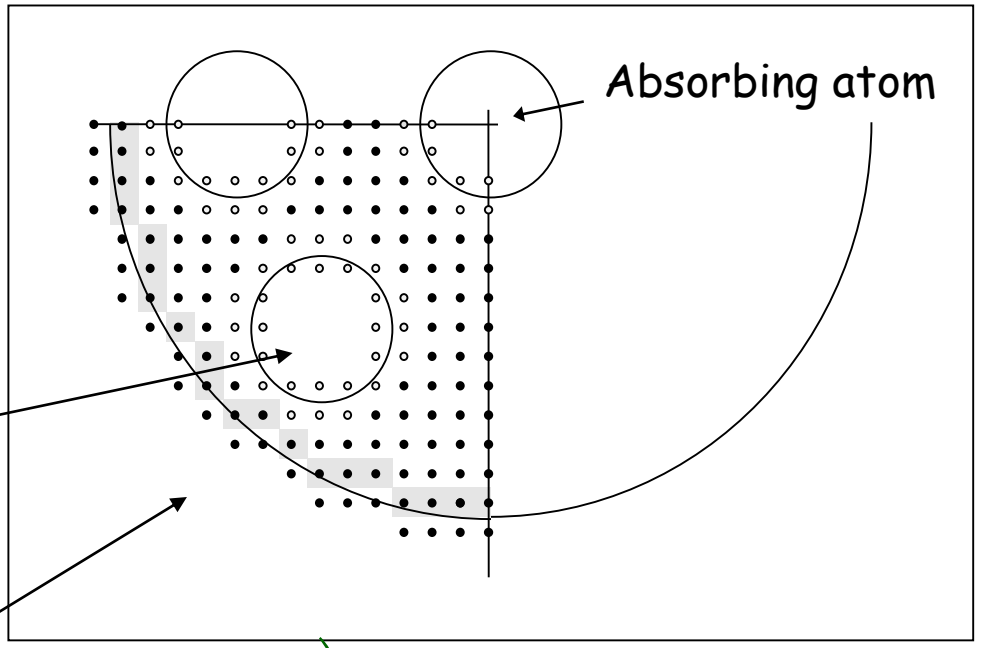

$$\varphi_f(\boldsymbol{r}) = \sum_{\ell m} a_{\ell m}^f(E_f) b_\ell(r, E_f) Y_\ell^m(\hat{r}) \chi_{\sigma_f}$$

$$\varphi_f(\boldsymbol{r}) = \sqrt{\frac{k}{\pi}}\left(j_{\ell_f}(kr) Y_{\ell_f}^{m_f}(\hat{r}) - i \sum_{\ell m} s_{\ell m}^f(E_f) h_\ell^+(kr) Y_\ell^m(\hat{r})\right)$$

+ continuity at area borders

Big matrix, unknowns: $\varphi_{f,i}$

Interest : free potential shape

Drawback : time consuming

→ Use of MUMPS library (sparse matrix solver)

→ 40 times faster → low symmetry possible

S. Guda, *et al.* J. Chem. Theory Comput. **11**, 4512 (2015)

Code for XANES using the mono-electronic approach (not complete)

C. R. Natoli (INFN, Frascati, Italy, 1980)	Cluster approach - Multiple scattering theory Now with a fit by M. Benfatto	CONTINUUM The first ! MXAN	
J. Rehr, A. Ankudinov *et al.* (Washington. U., USA, 1994)	Cluster approach - Multiple scattering theory - path expansion fit – self consistency	FEFF	feff.phys.washington.edu/feff/
T. Huhne, H. Ebert (München U., Germany)	Band structure approach – Full potential	SPRKKR	olymp.cup.uni-muenchen.de/ak/ebert/SPRKKR/
P. Blaha *et al.* (Wien, Austria)	Band structure, FLAPW	Wien-2k	susi.theochem.tuwien.ac.at
Y. Joly, O. Bunau (CNRS, Grenoble)	Cluster approach, MST and FDM	FDMNES	www.neel.cnrs.fr/fdmnes
K. Hermann, L. Pettersson (Berlin, Stockholm)	LCAO	STOBE	w3.rz-berlin.mpg.de/~hermann/StoBe/
D. Cabaret *et al.* (LMPC, Paris)	Band structure, Pseudo potential	Xspectra / Quantum-espresso	www-ext.impmc.jussieu.fr/~cabaret/xanes.html

Examples in XANES

Linear dichroism in rutile TiO_2

Experiment by Poumellec et al.

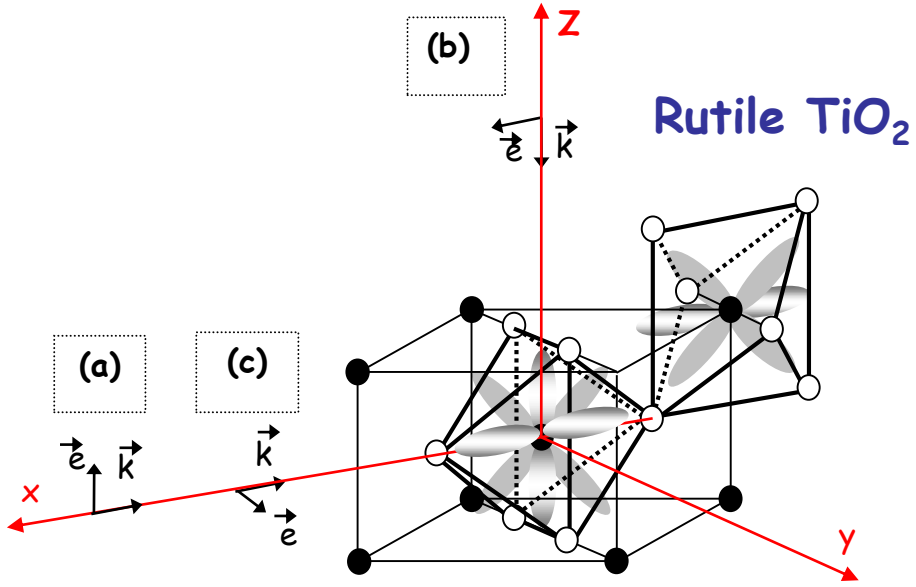

Influence of the core-hole

Shift of the 3d

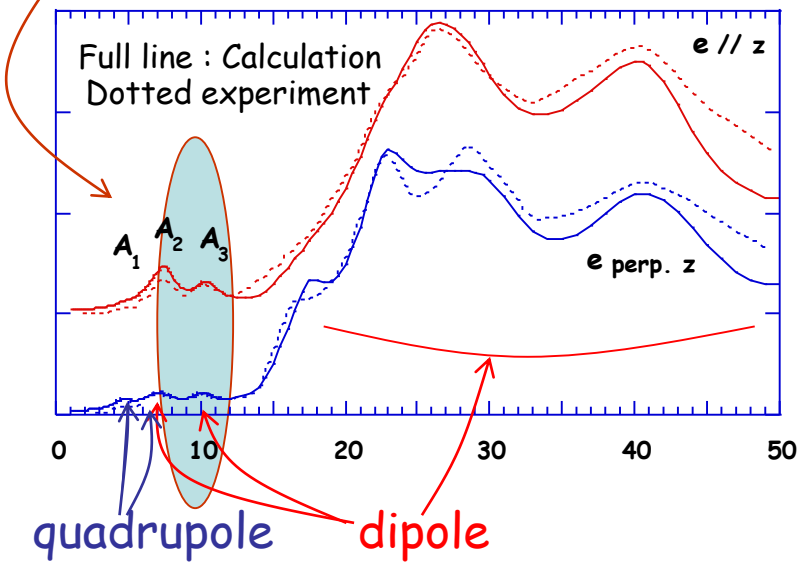

Important linear dichroism

Quantitative analysis of the pre-edge

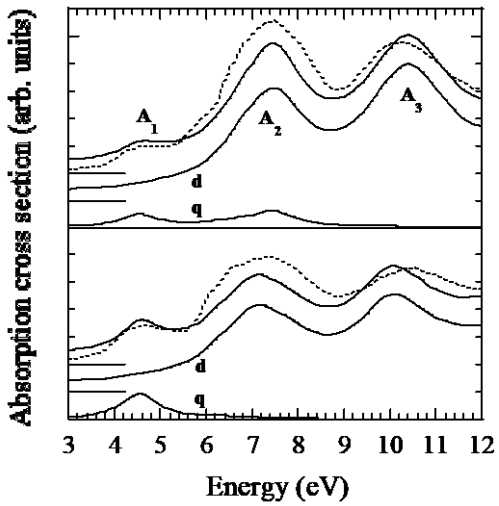

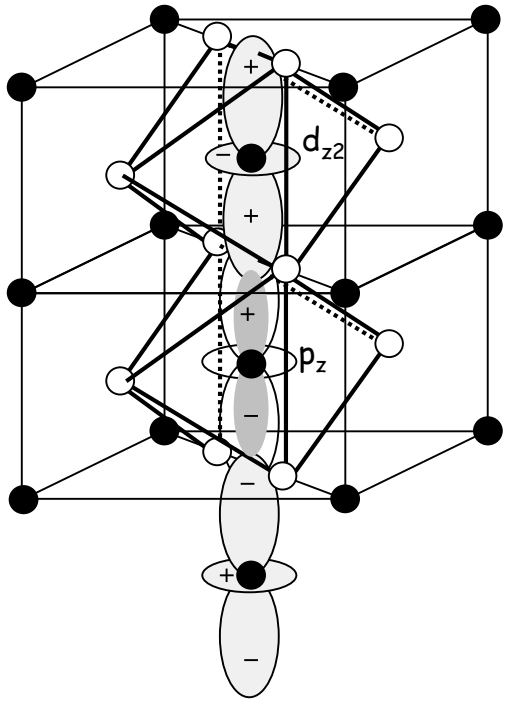

By the dipole component which probes the *p* states, we also observe the projection of the *d* states of the neighboring Ti

With a precise analysis of the XANES features, we get a detailed description of the electronic structure

Organic molecule on surface : acrylonitrile

For the light element

- Long hole life time
- Good energy resolution
- Study of the first non occupied molecular orbitals

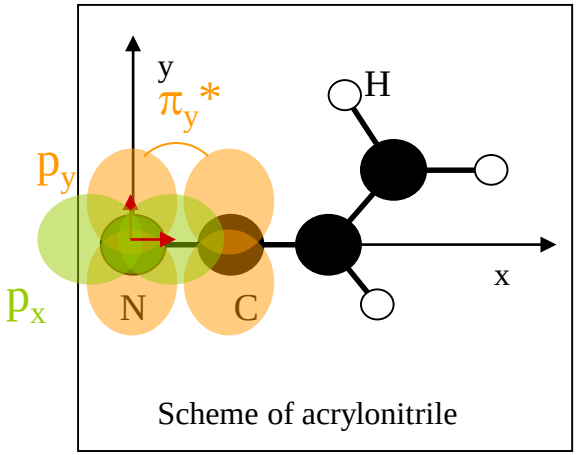

Scheme of acrylonitrile

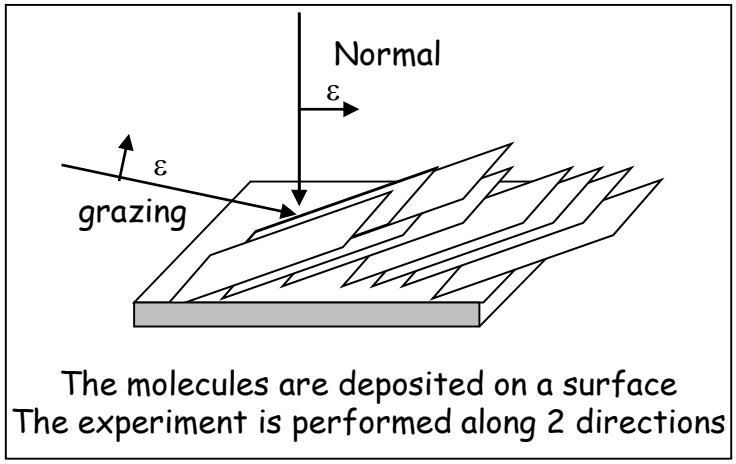

The molecules are deposited on a surface
The experiment is performed along 2 directions

Normal incidence, x-ray probe p_x and p_y orbitals, projections of the antibonding molecular orbitals π_y* and s

Grazing incidence, x-ray probe p_z orbitals, projections of the antibonding molecular orbitals π_z*

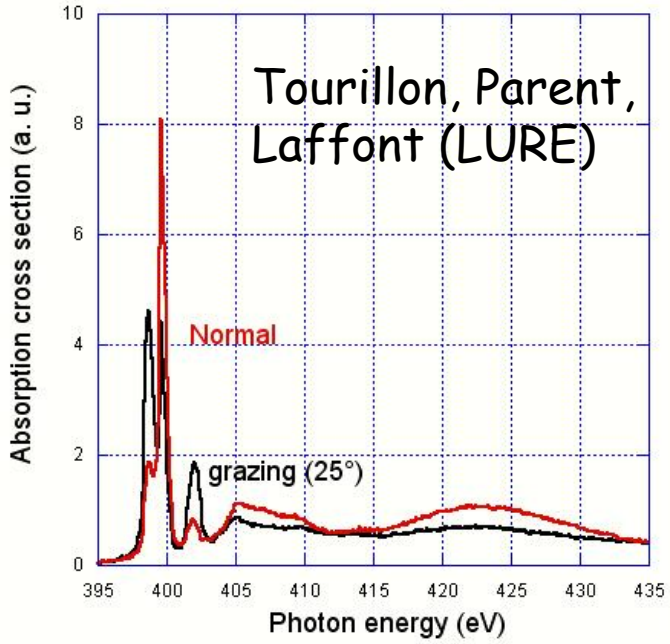

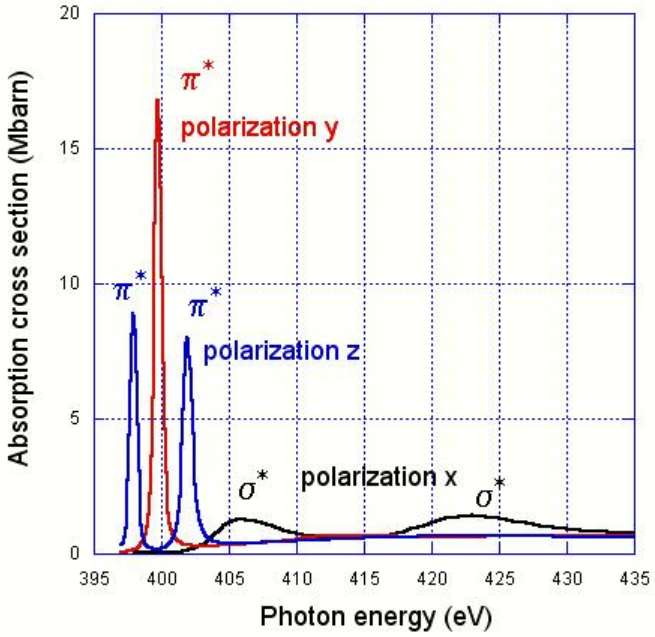

Normal = $\frac{1}{2}\cos\theta(\sigma_x+\sigma_y)+\sin\theta\sigma_z$

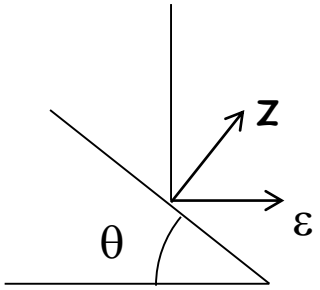

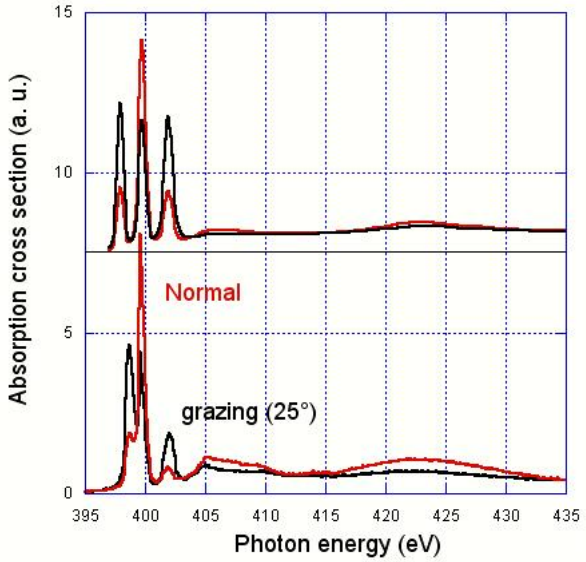

XANES lets to determine how are arranged the molecules

H_2O gaz

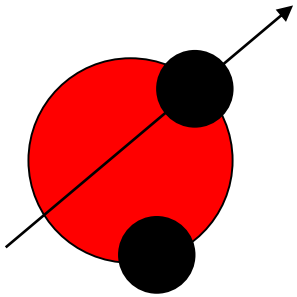

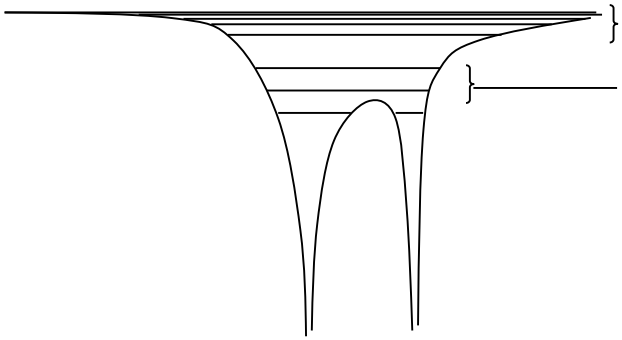

Unoccupied
bound states

Experiment

Calculation

(without broadening)

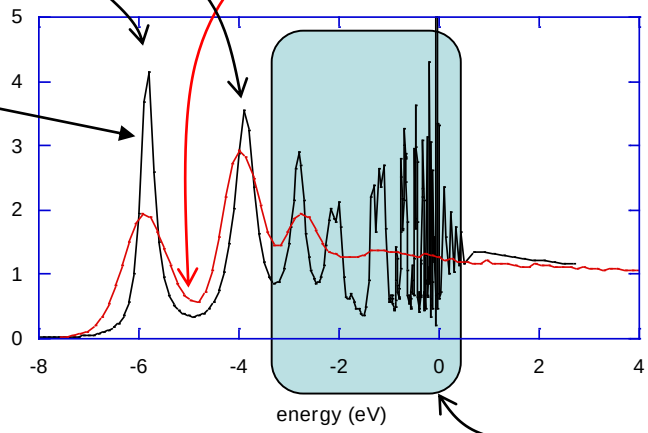

Rydberg
series

Iron in solution

With Wang and Vaknin, Ames Laboratory

Fe^{2+} → Fe-O = 2.16 A
Fe^{3+} → Fe-O = 2.06 A

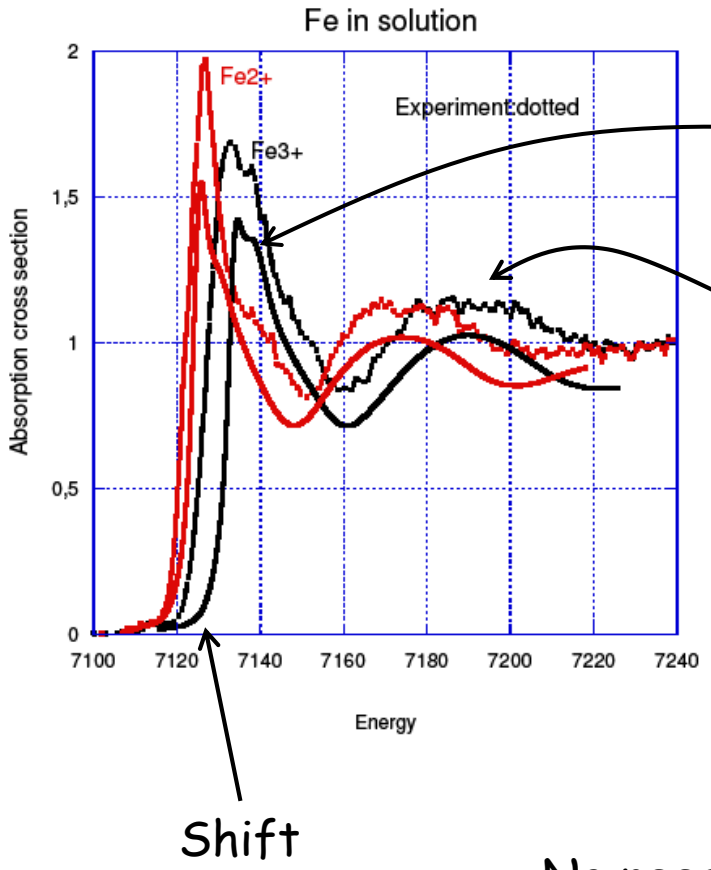

shoulder

Effect of second shell

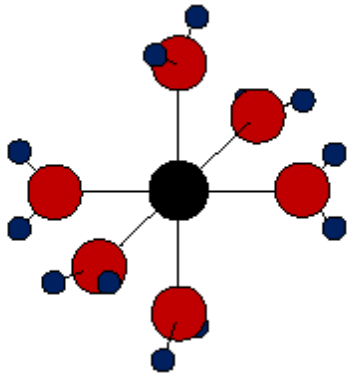

Shift

No need of mixing Fe^{2+} - Fe^{3+}

X-ray linear dichroism of (Fe,N) co-doped TiO_2

T. C. Kaspar, A. Ney *et al.*

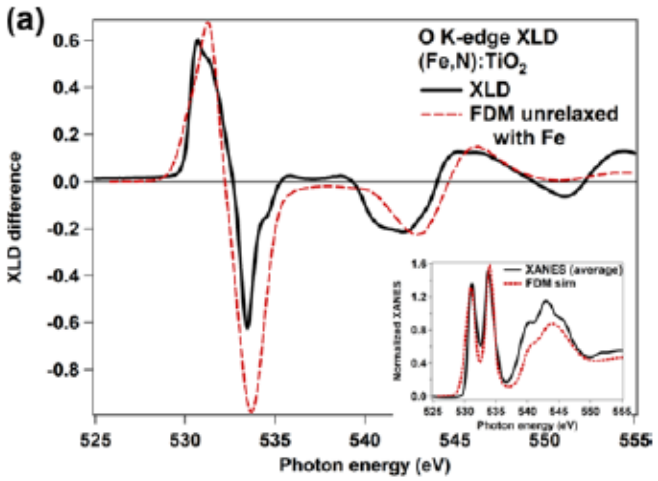

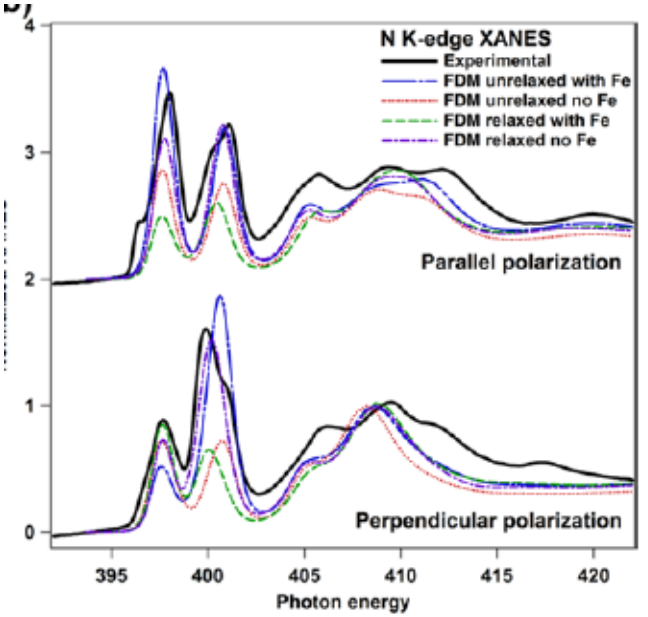

Exp: ID08 / ESRF

Need of full potential + SCF

Care with molecular dynamic relaxed structure

PRB 2012

XMCD study in RZn compounds at the L_{23} edges

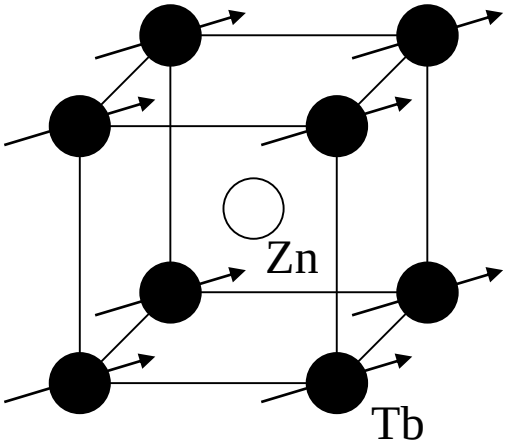

With R.-M. Galera, A. Rogalev, N. Binggeli

Work with LSDA+U

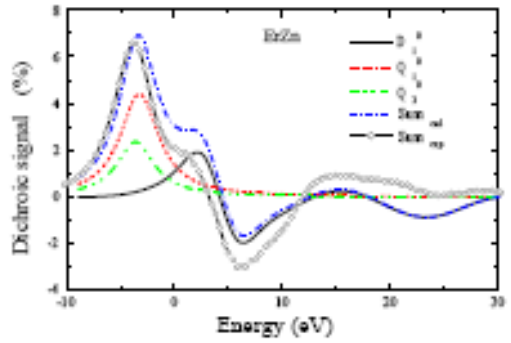

Figure 4: (color online) Summation over the L_2 and L_3 edges of the calculated (dash dot line) and experimental (open circles) dichroic signal in ErZn. The contibution of the different components, D_1^2 (solid line), Q_1^2 (dashed line) and Q_3^0 (dash dot dot line) to the calculated signal are also reported. The Q_1^2 component related to the $4f$ orbital magnetic moment along z, is the dominant contribution to the signal.

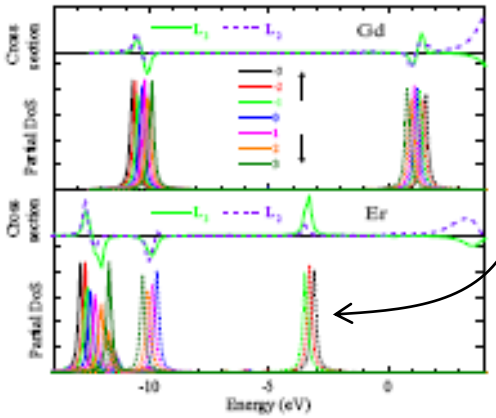

Figure 5: (color online) ErZn and GdZn compounds: upper part, calculated dichroic cross section for the (E2-E2) and (E1-E1) processes at the L_2 (dashed lines) and L_3 (solid lines) edges. Lower part, partial density of states for the $4f$ orbitals. The spin-orbit coupling spreads the different $4f$ states.

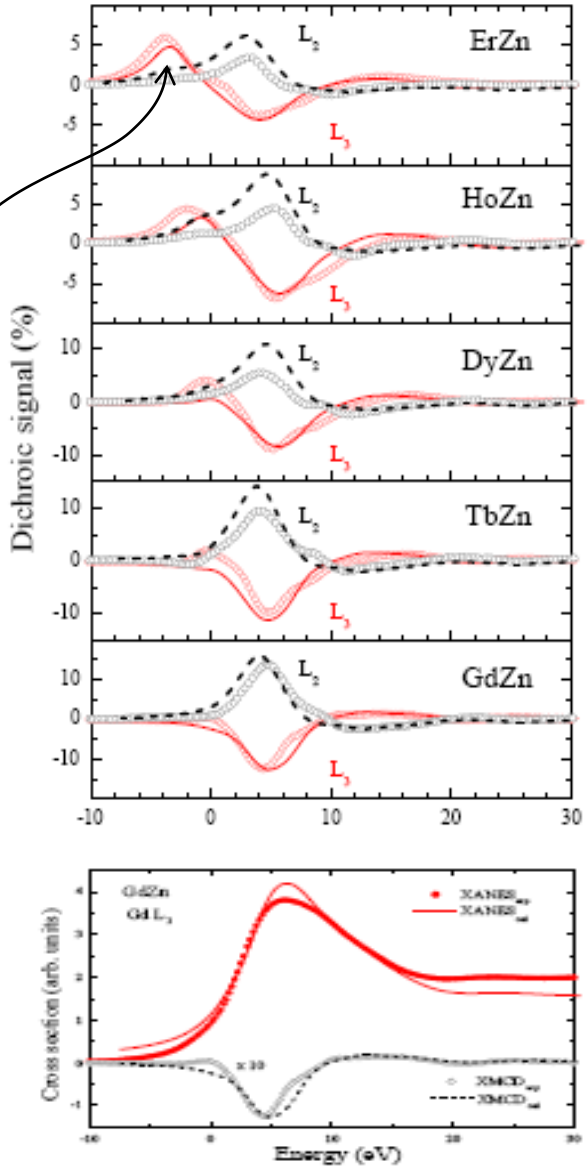

X-ray directional dichroism of a polar ferrimagnet

With S. Di Matteo

$GaFeO_3$ M. Kubota et al., Phys. Rev. Lett. **92**, 137401 (2004)

Space group : $Pc2_1n$
Magnetic point group : $m'2'm$
$Tc \approx 205$ K

Magnetic field along c : +/-

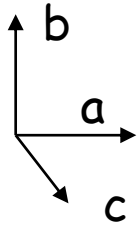

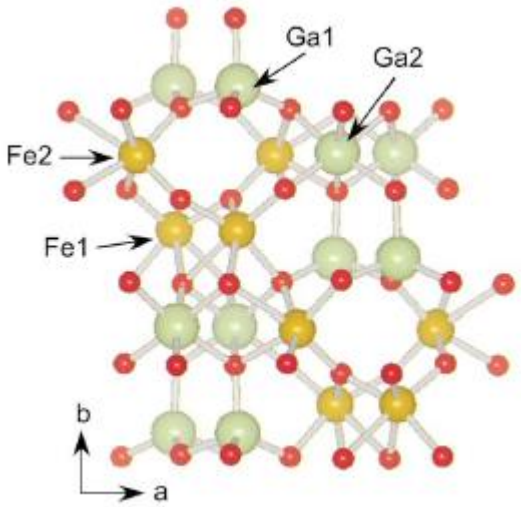

(1) Polarization along b

$$\sigma_b^+ - \sigma_b^- \propto \mathrm{Im}\left(p_y d_{xy}\right)$$

(2) Polarization along c

$$\sigma_c^+ - \sigma_c^- \propto \mathrm{Im}\left(p_z d_{xz}\right)$$

Dipole-dipole (*p* density of state),
Quadrupole-quadrupole (*d* density of state),
Real part of dipole-quadrupole (natural dichroism) are eliminated…

⟶ Measurement of the toroidal moment…(non reciprocal activity)

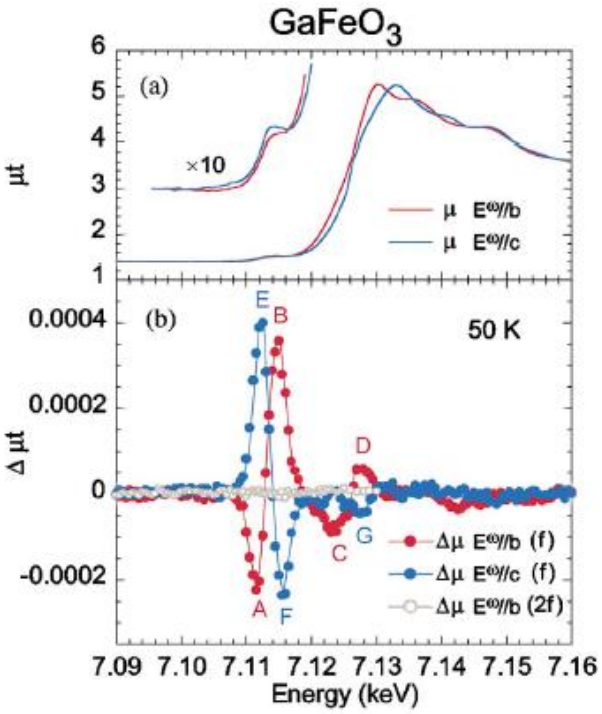

FIG. 2 (color). Spectra of (a) the x-ray absorption μt and (b) the XNDD $\Delta\mu t$ of a $GaFeO_3$ crystal at 50 K for $E^\omega \parallel b$ (red) and $E^\omega \parallel c$ (blue). $\Delta\mu t$ is defined as the difference of absorption coefficients when a magnetic field is applied parallel $(H+)$ and antiparallel $(H-)$ to the c axis. In (b) the spectrum of the second-harmonic component of the magnetic-field modulation for $E^\omega \parallel c$ is also shown with open circles.

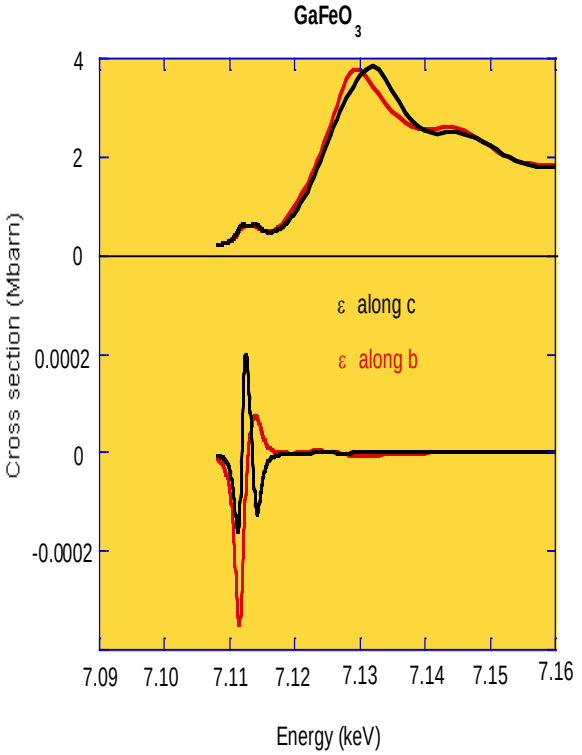

Even with a relatively crude calculation, it is possible to check the origin of very thin experimental features !

Pt_{13} cluster on γ-Al_2O_3 under H_2

A. Gorczyca *et al.*, coll. IFPEN, Solaize, France
J.-L. Hazemann, O. Proux…

Many parameters
- 13 Pt positions
- H number
- H positions
- 2 difference faces
- Some size dispersion
- Several site absorption…

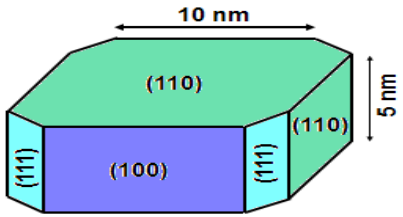

Exp: FAME / ESRF

High resolution XANES
+
DFT-Molecular dynamics (VASP)
+
XANES simulation

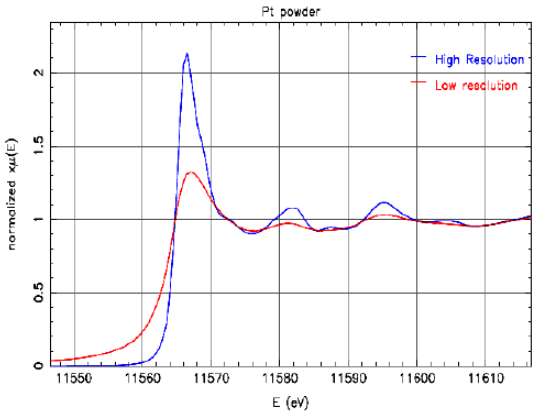

Fig. 2 : Pt L_3 HERFD XANES spectrum (blue) compared to classical fluorescence XANES spectrum (red) of 20 wt% Pt powder in BN.

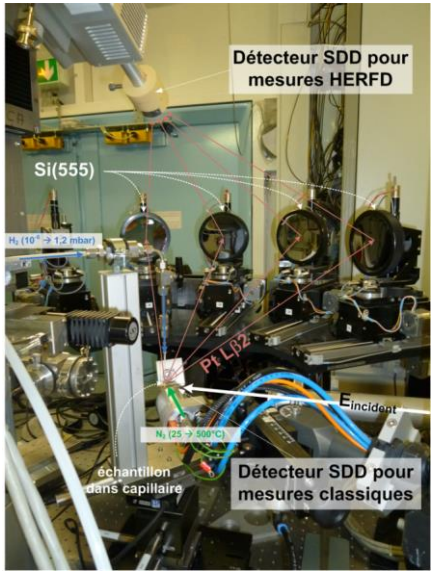

Experimental observations

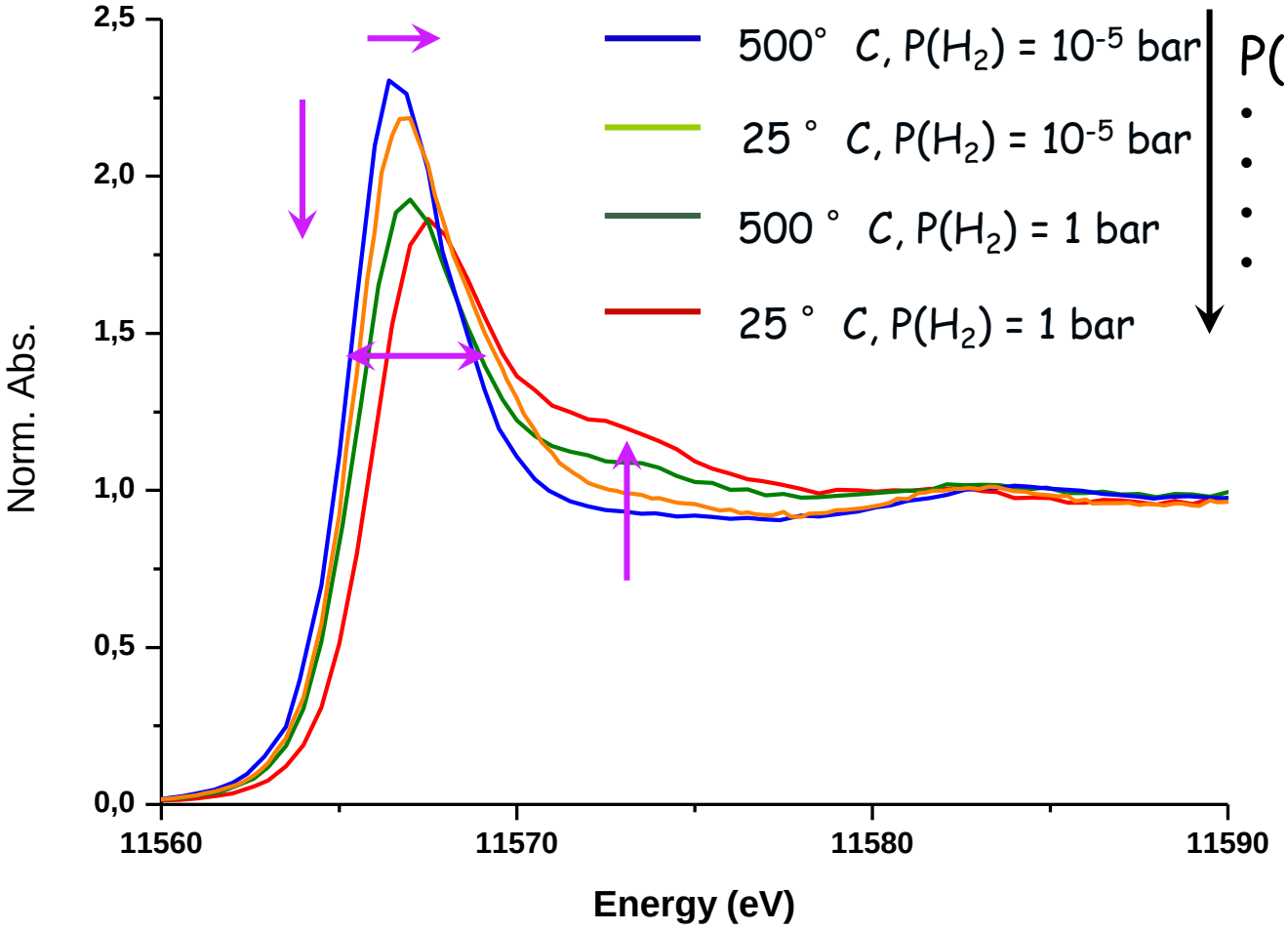

$P(H_2)$ ↗ or T ↘:

- ↘ intensity of white line
- WL wider
- Energy shift
- ↗ post white line features

Pt_{13} / γ – alumina case

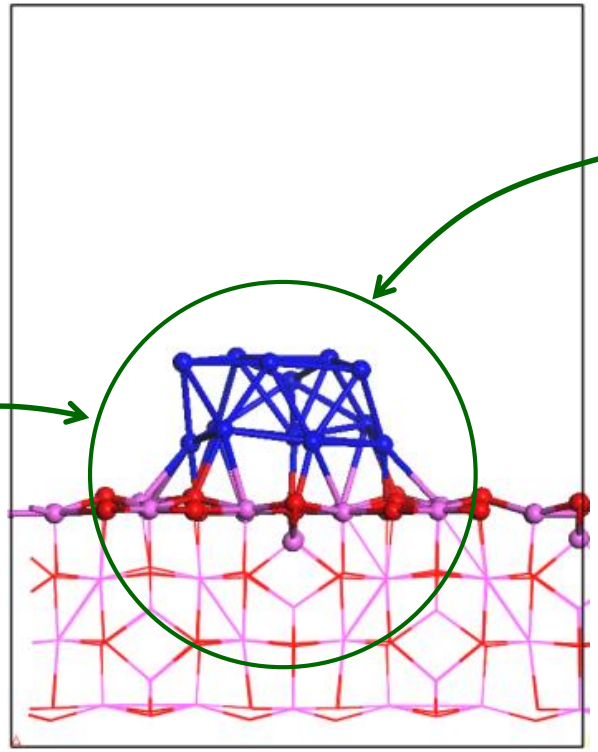

Set of atomistic models from DFT (VASP)

Area of calculation containing the Pt (H) cluster and substrate (distorted) atoms

L_3 simulation in the ground state

1 calculation gives the 13 atoms absorption spectra

MST

Spectra sensitivity on models

(100) face only

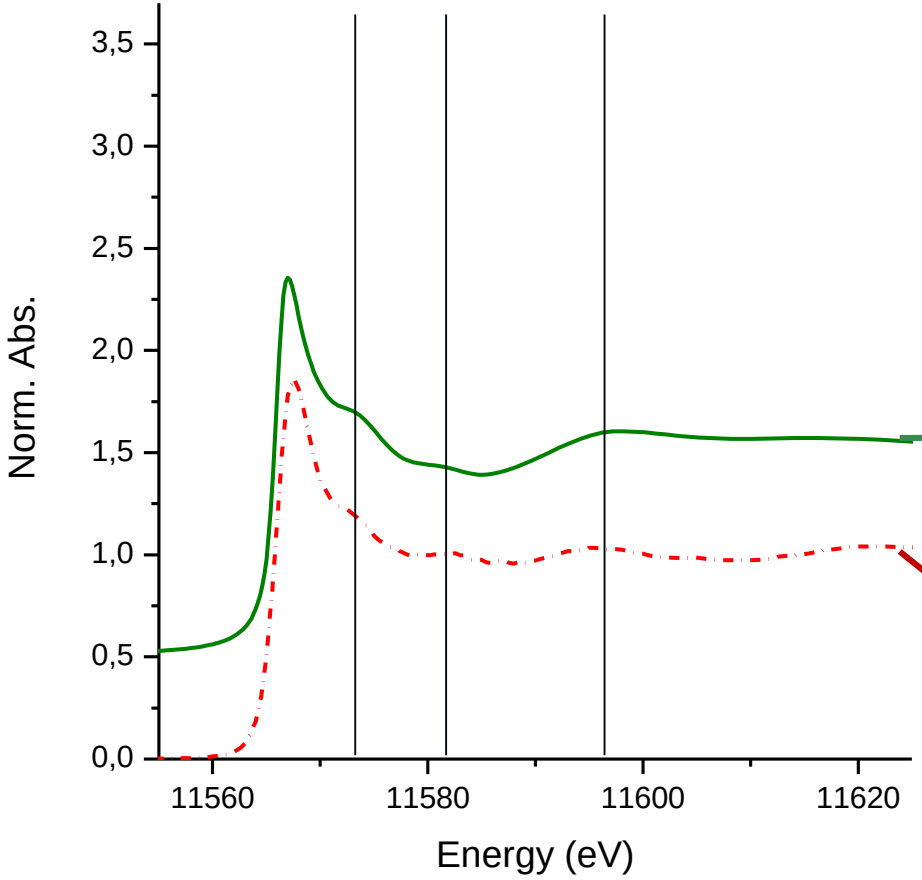

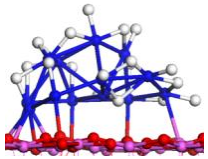

18 H

Experimental spectrum
25° C, P(H_2) = 1bar

Spectra sensitivity on models

(100) face only

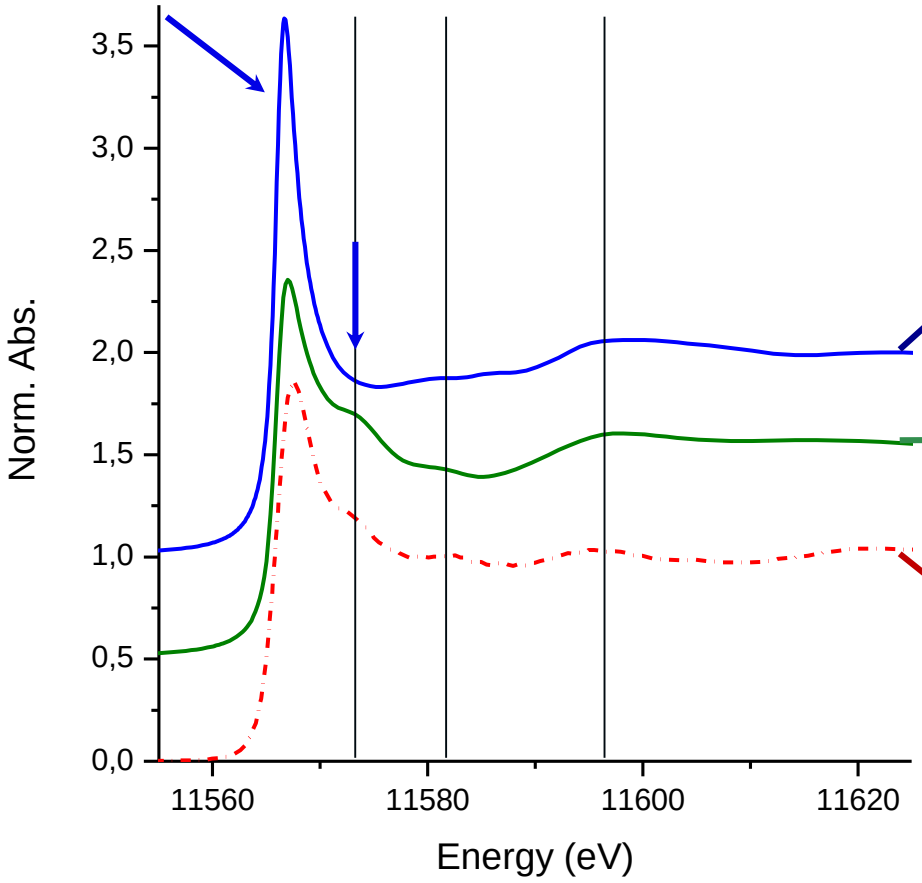

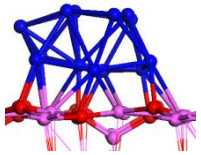

0 H

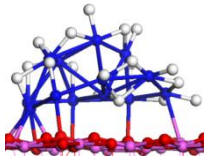

18 H

Experimental spectrum
25° C, $P(H_2)$ = 1bar

Spectra sensitivity on models

(100) face only

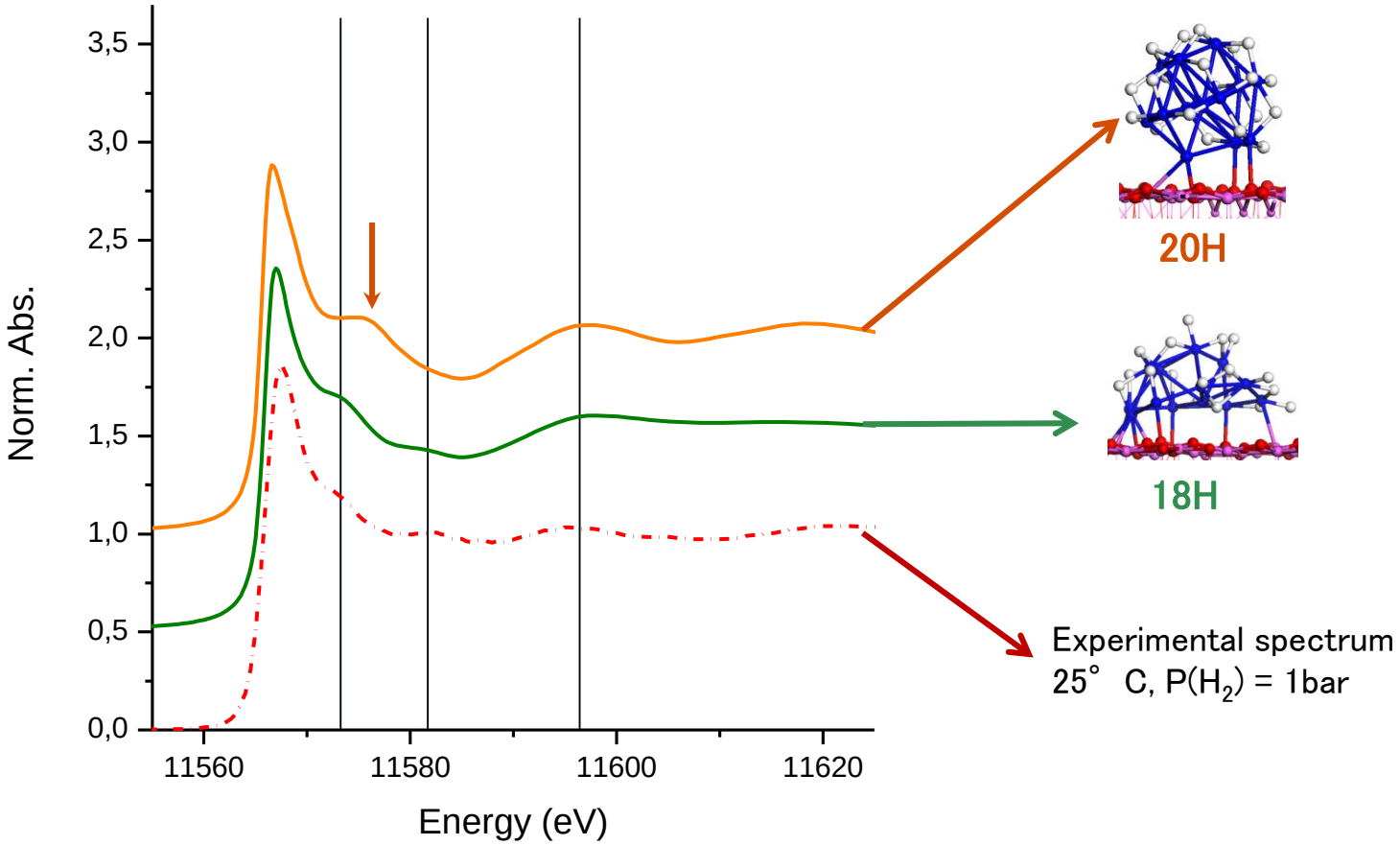

Sensitive tool for the quantification of hydrogen coverage and morphology

Simulations vs experiments :
Best fits

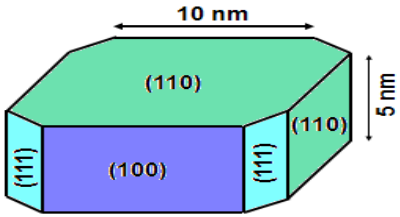

(110)

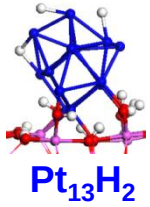

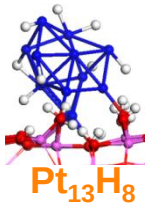

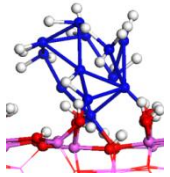

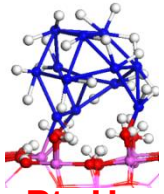

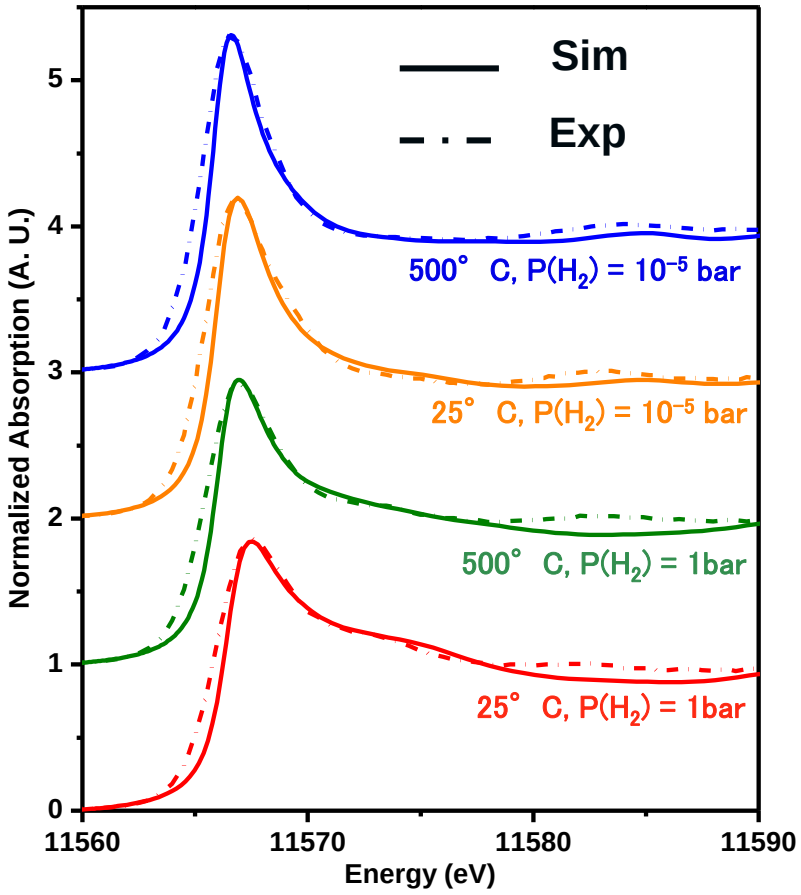

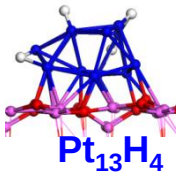

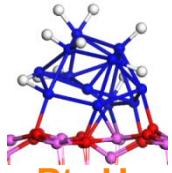

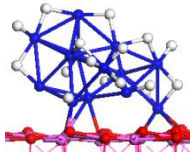

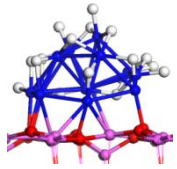

(100)

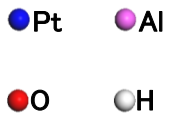

Identification of hydrogen coverage / morphology on each surface and for each experimental condition

A. Gorczyca *et al.* Angew. Chem. Int. Ed., **53**, 12426 (2014)

X-ray Raman Scattering

X-ray Raman Scattering (XRS)

or Non Resonant X-ray Inelastic Scattering (or EELS on Trans. Elec. Micr.)

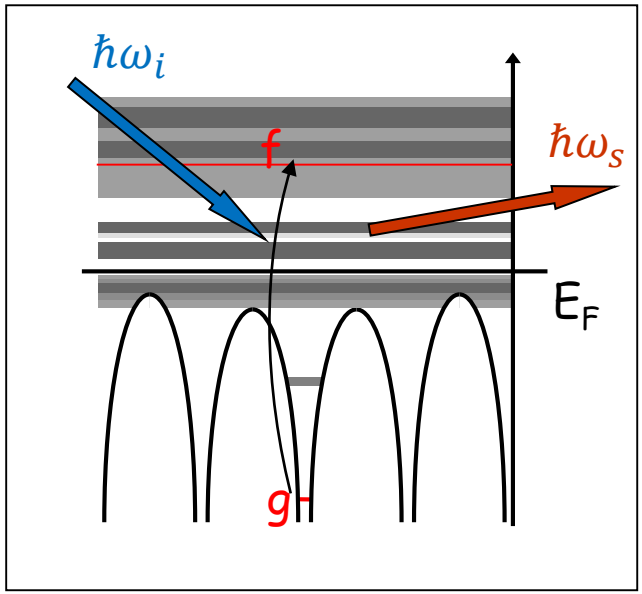

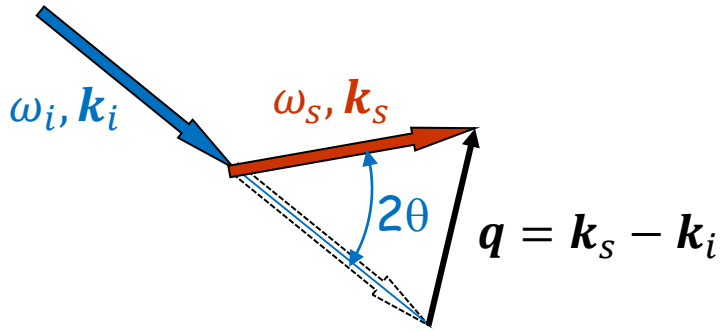

Inelastic scattering technique
→ energy loss ≈ absorption edge energy

$$\hbar\omega = \hbar\omega_s - \hbar\omega_i = E_f - E_g$$

First experiments by Suzuki et al. (end of 60th)

Main interest → access to low energy edges using hard X-ray
in situ, operando, extreme conditions…
Drawback → low signal

But new synchrotron generation, new spectrometers
→ new XRS beamlines

The formula

Cross section:

$$\frac{d^2\sigma}{d\Omega_s d\hbar\omega_s} = r_0^2 \frac{\omega_s}{\omega_i} |\varepsilon_s . \varepsilon_i|^2 S(\boldsymbol{q}, \omega)$$

Dynamic structure factor:

$$S(\boldsymbol{q}, \omega) = \sum_{f,g} \left|\langle f \left| e^{-i\boldsymbol{q}.\boldsymbol{r}} \right| g \rangle\right|^2 \delta\left(\hbar\omega - \left(E_f - E_g\right)\right)$$

First approximation : $\left|\langle f \left| e^{-i\boldsymbol{q}.\boldsymbol{r}} \right| g \rangle\right|^2 \cong |\langle f | 1 - i\boldsymbol{q}.\boldsymbol{r} | g \rangle|^2 \cong |\langle f | \boldsymbol{q}.\boldsymbol{r} | g \rangle|^2$

Same than (dipole) XANES, with ε → q

Exact expansion: $e^{-i\boldsymbol{q}.\boldsymbol{r}} = 4\pi \sum_{\ell m} (-i)^\ell j_\ell(qr)\, Y_\ell^{m*}(\hat{r}) Y_\ell^m(\hat{q})$

Bessel function

$$e^{-i\boldsymbol{q}.\boldsymbol{r}} = 4\pi \sum_{\ell m} (-i)^{\ell} j_{\ell}(qr)\, Y_{\ell}^{m*}(\hat{r}) Y_{\ell}^{m}(\hat{q})$$

$$S(\boldsymbol{q},\omega) = \sum_{f,g} |\langle f | j_0(qr) - 4\pi i j_1(qr) \textstyle\sum_m Y_1^{m*}(\hat{r}) Y_1^{m}(\hat{q}) + \cdots | g \rangle|^2 \delta\left(\hbar\omega - \left(E_f - E_g\right)\right)$$

Comparison with XANES:

$$\sigma(\omega) = 4\pi^2 \alpha \hbar \omega \sum_{fg} |\langle f | \boldsymbol{\varepsilon} \cdot \boldsymbol{r} + \cdots | g \rangle|^2 \delta\left(\hbar\omega - E_f + E_g\right)$$

$$\boldsymbol{\varepsilon} \cdot \boldsymbol{r} = \frac{4\pi}{3} r \sum_m Y_1^{m*}(\hat{r}) Y_1^{m}(\hat{\varepsilon})$$

$$\sigma(\omega) = 4\pi^2 \alpha \hbar \omega \sum_{fg} \left| \left\langle f \left| \frac{4\pi}{3} r \textstyle\sum_m Y_1^{m*}(\hat{r}) Y_1^{m}(\hat{\varepsilon}) + \cdots \right| g \right\rangle \right|^2 \delta\left(\hbar\omega - E_f + E_g\right)$$

$$\sigma(\omega) = 4\pi^2\alpha\hbar\omega \sum_{fg} \left|\left\langle f\left|\frac{4\pi}{3} r \sum_m Y_1^{m*}(\hat{r}) Y_1^m(\hat{\varepsilon}) + \cdots\right|g\right\rangle\right|^2 \delta(\hbar\omega - E_f + E_g)$$

$$S(\boldsymbol{q},\omega) = \sum_{f,g} |\langle f|j_0(qr) - 4\pi i j_1(qr) \sum_m Y_1^{m*}(\hat{r}) Y_1^m(\hat{q}) + \cdots |g\rangle|^2 \delta\left(\hbar\omega - \left(E_f - E_g\right)\right)$$

$$\frac{\sin qr}{qr} \qquad -\frac{\cos qr}{qr} + \frac{\sin qr}{(qr)^2}$$

$$\approx 1 - \tfrac{1}{6}(qr)^2 \qquad \approx \tfrac{1}{3}qr$$

Monopole
$\Delta\ell = 0$

Dipole
$\Delta\ell = \pm 1$

selection rule from:

$$\int Y_{\ell_f}^{m_f *}(\hat{r})\, Y_\ell^{m*}(\hat{r}) Y_{\ell_g}^{m_g}(\hat{r}) d\hat{r} \neq 0$$

→ Dependence on **q** (scat. angle)

→ Probe of the different ℓ

Disordered material case (powder)

$$S(\boldsymbol{q},\omega) = \sum_{f,g} \left|\langle f \left| 4\pi \sum_{\ell m} (-i)^{\ell} j_{\ell}(qr)\, Y_{\ell}^{m*}(\hat{r}) Y_{\ell}^{m}(\hat{q}) \right| g \rangle\right|^2 \delta\left(\hbar\omega - \left(E_f - E_g\right)\right)$$

$$S(q,\omega) = \int \sum_{f,g} \left|\langle f \left| 4\pi \sum_{\ell m} (-i)^{\ell} j_{\ell}(qr)\, Y_{\ell}^{m*}(\hat{r}) Y_{\ell}^{m}(\hat{q}) \right| g \rangle\right|^2 \delta\left(\hbar\omega - \left(E_f - E_g\right)\right) d\hat{q}$$

⟶

$$S(q,\omega) = (4\pi)^2 \sum_{\ell m} \sum_{f,g} |\langle f | j_{\ell}(qr) Y_{\ell}^{m*}(\hat{r}) | g \rangle|^2 \delta\left(\hbar\omega - \left(E_f - E_g\right)\right)$$

No crossing term (Q0-Q1, Q0-Q2, Q1-Q2…)

Examples

F edge in LiF

Cubic
$Fm\bar{3}m$

Pt. group
$m\bar{3}m$

SCF
R = 8 Å

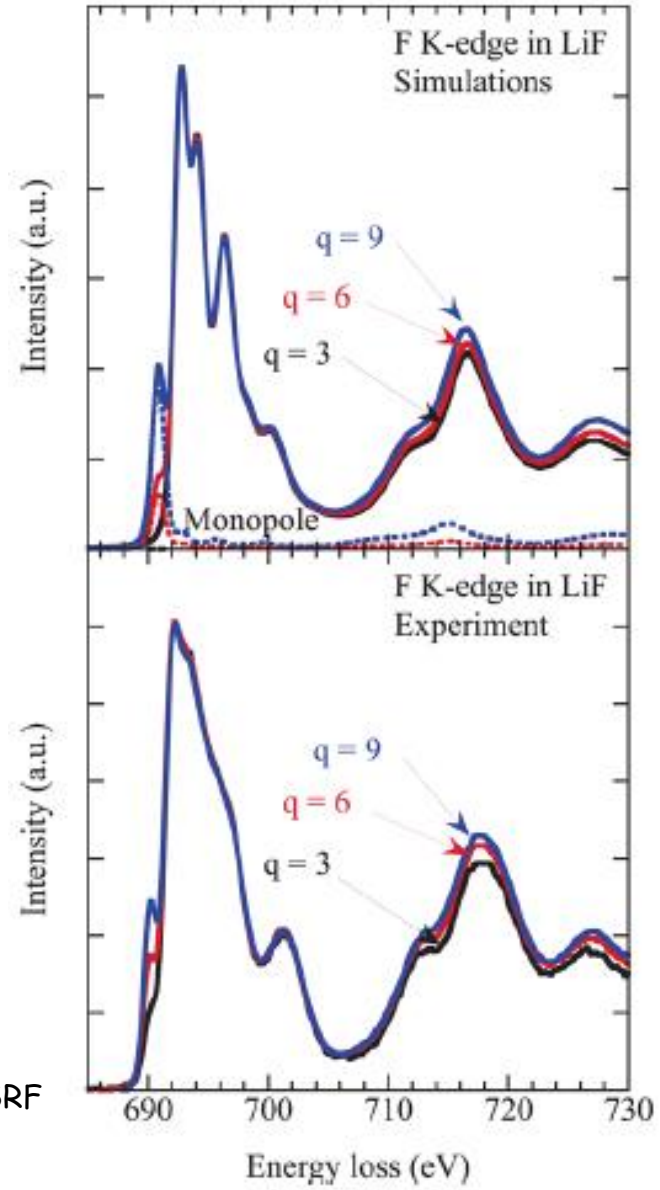

Exp
ID20, ESRF

Comparison with muffin-tin approx.

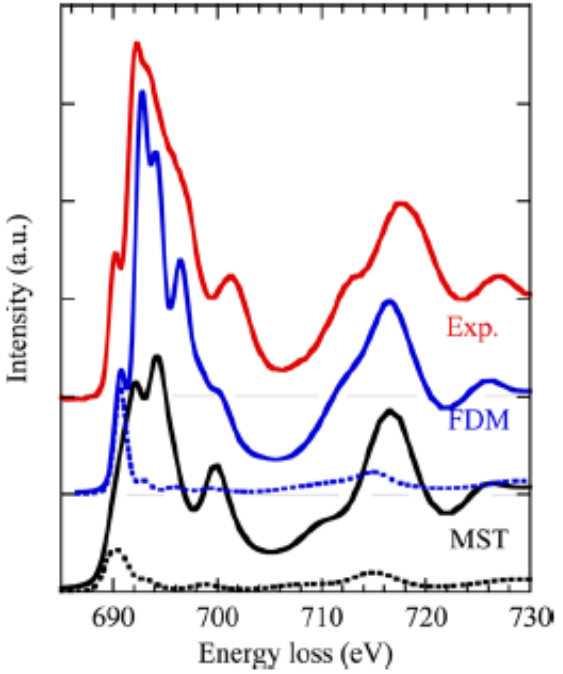

h-BN

Sp. group
P63/mmc

Pt. group
$\bar{6}$m2

SCF
R = 8 Å (B)
R = 10 Å (N)

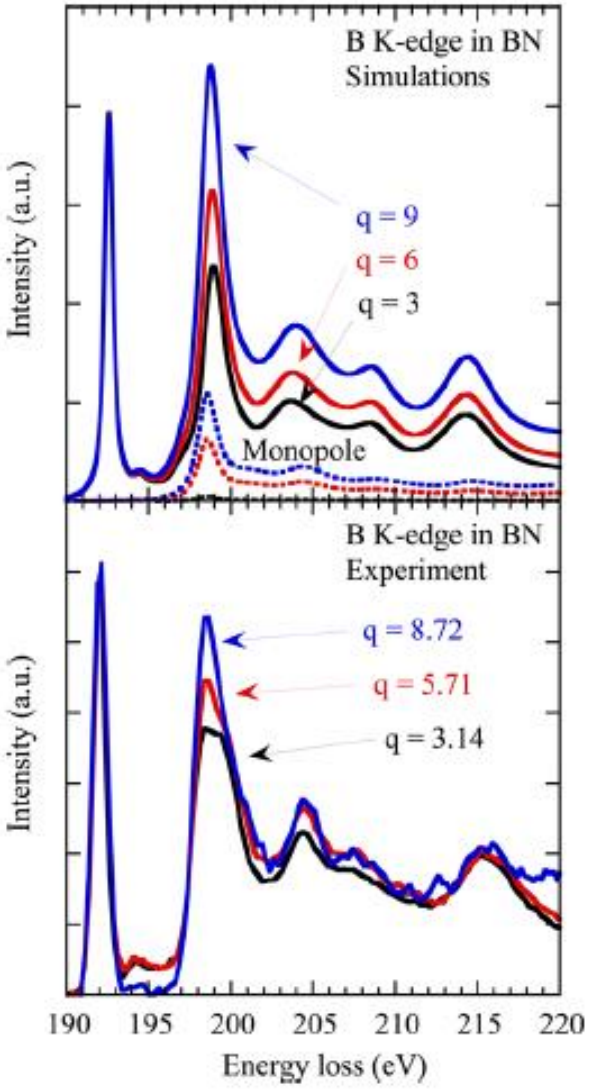

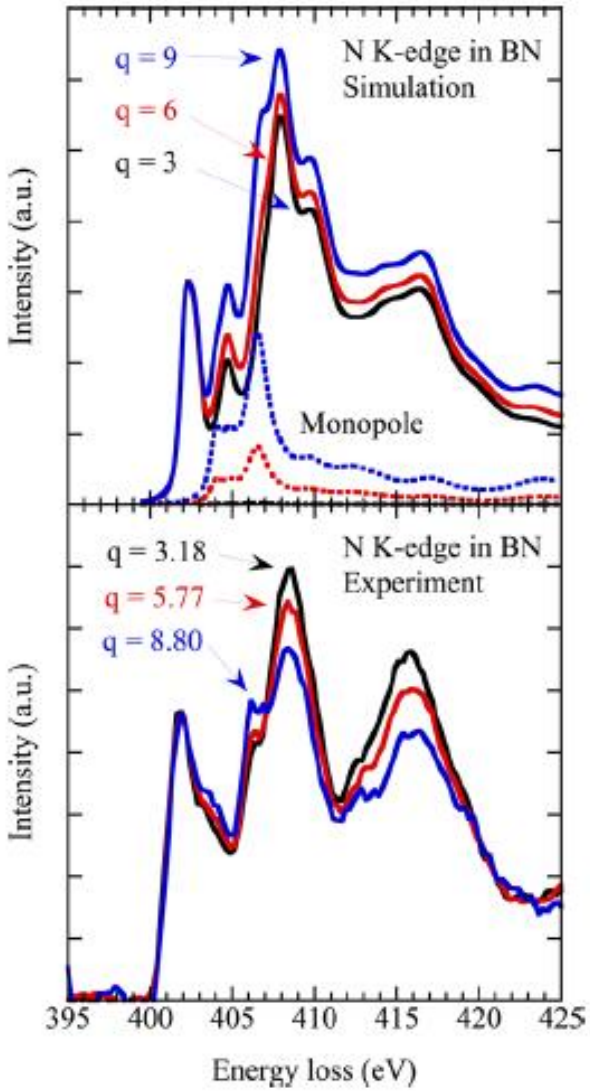

3-fold axis along c
→ sp^2 in basal plane

m plane
→ no $p_z - s$ hybridization

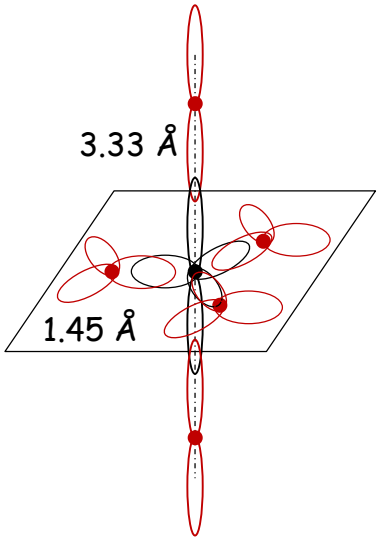

Anti-bonding
$\mathrm{B}sp^2 - \mathrm{N}sp^2$
$\mathrm{B}p_z - \mathrm{N}p_z$

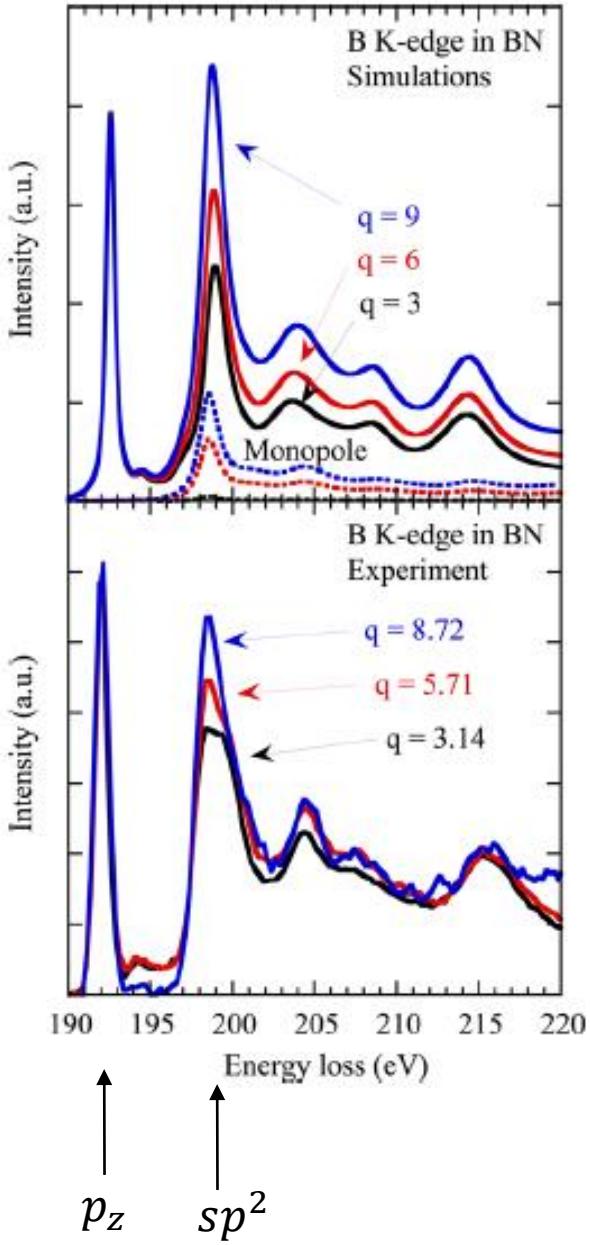

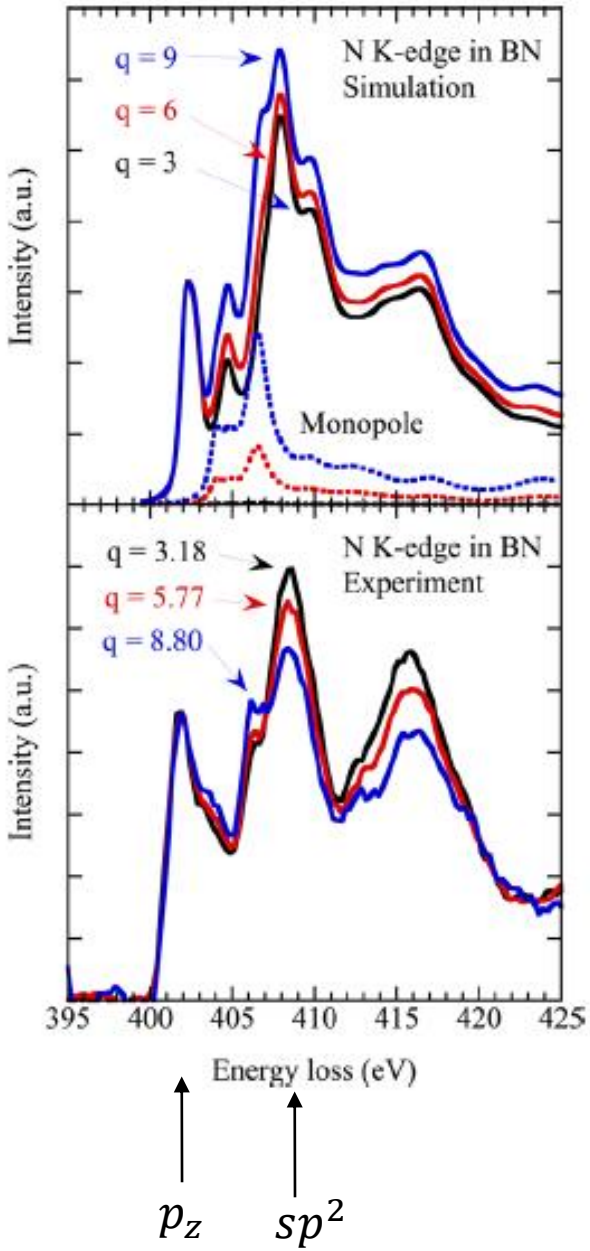

Y. Joly, C. Cavallari, S. A. Guda, and C. J. Sahle,
J. Chem. Theory Comput. **13**, 2172-2177 (2017).
DOI: 10.1021/acs.jctc.7b00203

Resonant X-ray diffraction

Variation of diffracted peak intensities around absorption edges known from the 1920th…

First spectra : Yvette Cauchois (1956)

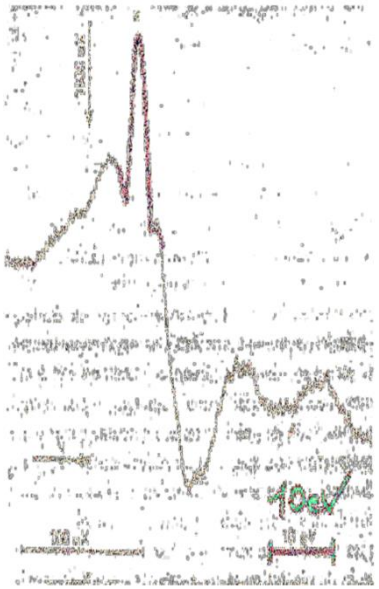

(002) Reflection
around Al K edge in mica

Y. Cauchois. Distribution spectrale observée dans une région d'absorption propre de divers cristaux. *Comptes Rendus de l'Academie des Sciences (Paris)*, 242 :100–102, 1956.

Relation between X-ray absorption and resonant diffraction

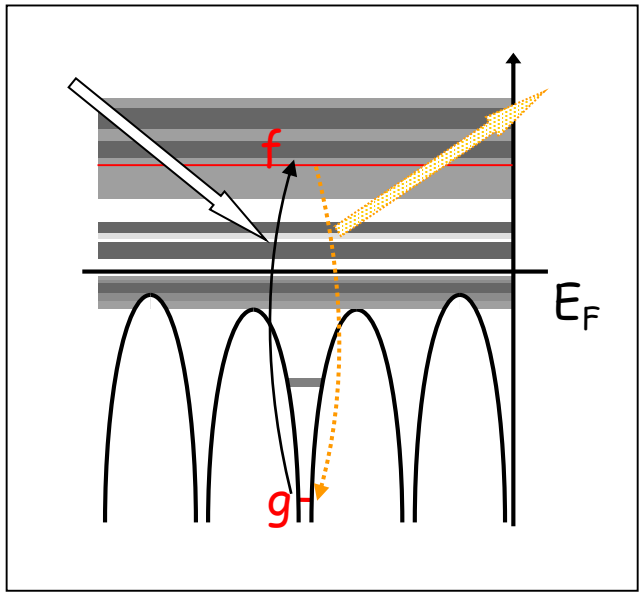

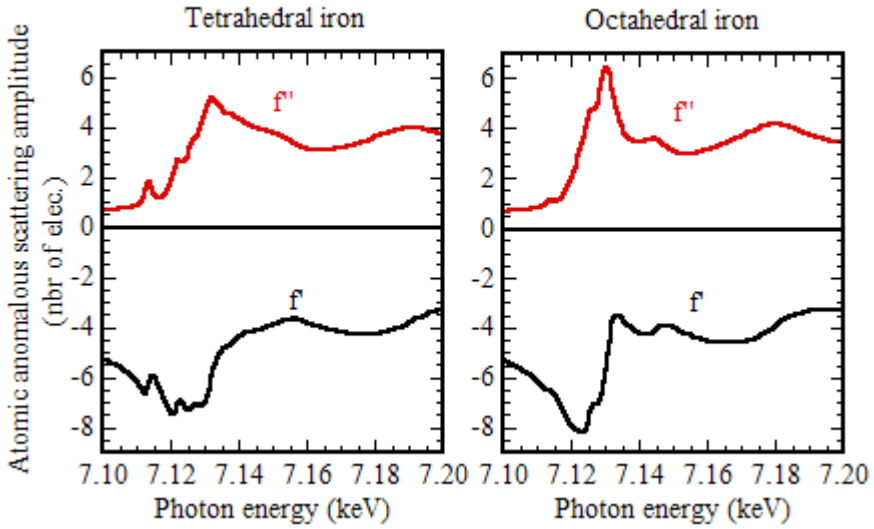

$$f'(\omega) - if''(\omega) = m\omega^2 \lim_{\eta \to 0^+} \sum_{fg} \frac{\langle g|o_s^*|f\rangle\langle f|o_i|g\rangle}{\hbar\omega - (E_F - E_g) + i\eta}$$

The imaginary part is proportional

to the absorption cross section

Summation over the atoms Bragg factor + Thomson (non resonant) term :

Magnetic non resonant term

$$I_Q(\omega) = \frac{K}{V^2}\left|\sum_a e^{-i\boldsymbol{Q}.\boldsymbol{R}_a}\left(f_{0a} - if_{ma} + f_a'(\omega) - if_a''(\omega)\right)\right|^2$$

Resonant term

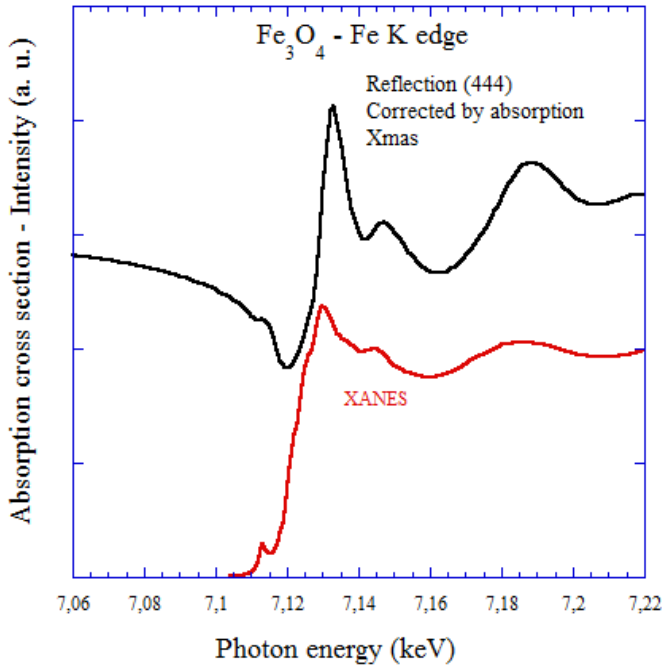

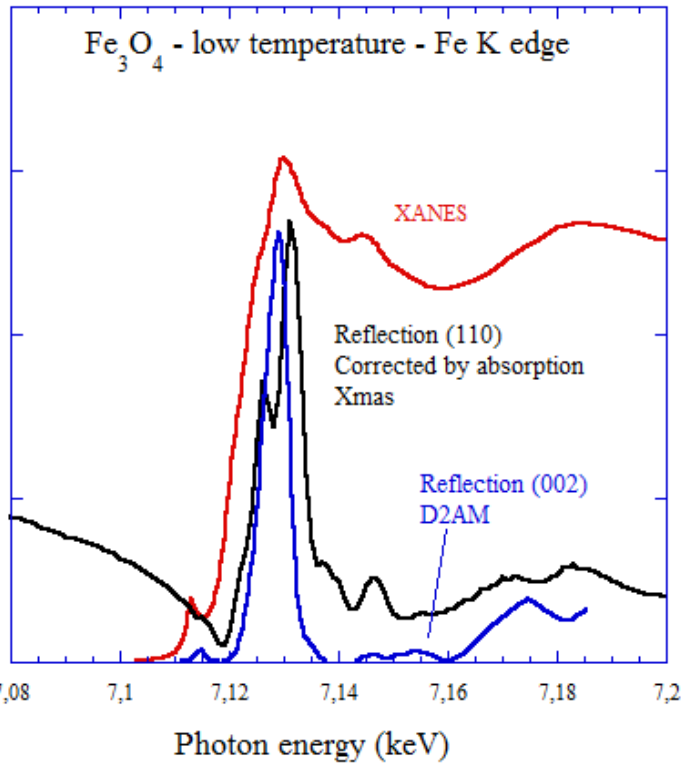

Special interest on the forbidden (or weak) reflections :

$$I_Q \approx |f_a - f_b|^2$$

More sensitive than XANES !

Polarization dependance

Acta Cryst. (1982). A**38**, 62–67

X-ray Dichroism and Polarized Anomalous Scattering of the Uranyl Ion

BY DAVID H. TEMPLETON AND LIESELOTTE K. TEMPLETON

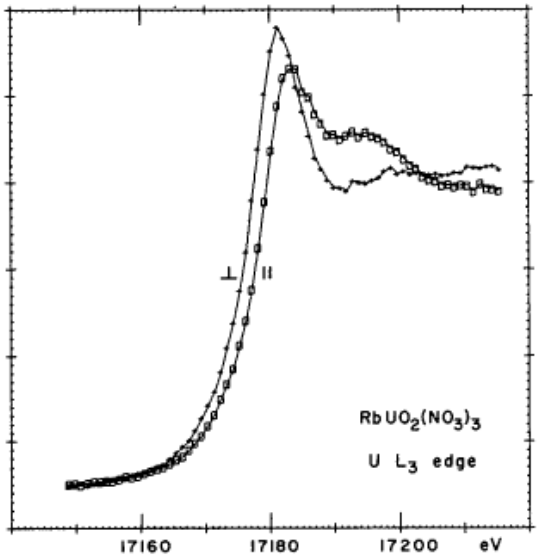

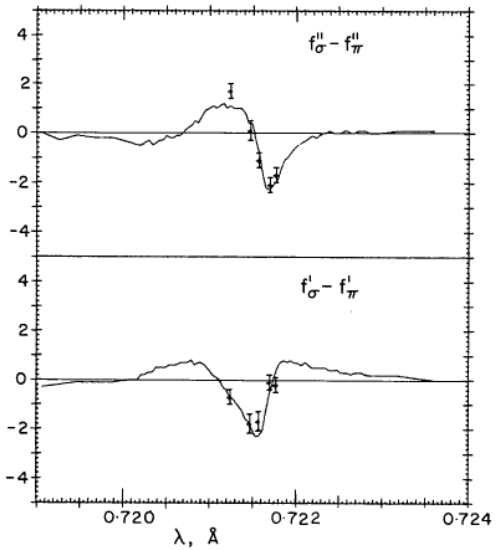

Fig. 4. Polarization anisotropy of f' and f'' for the uranyl ion near the L_3 edge, measured in the diffraction experiments (points with error bars) and the absorption experiment (continuous curves).

Forbidden reflections

Acta Cryst. (1983). A**39**, 29–35

Forbidden Reflections due to Anisotropic X-ray Susceptibility of Crystals

BY V. E. DMITRIENKO

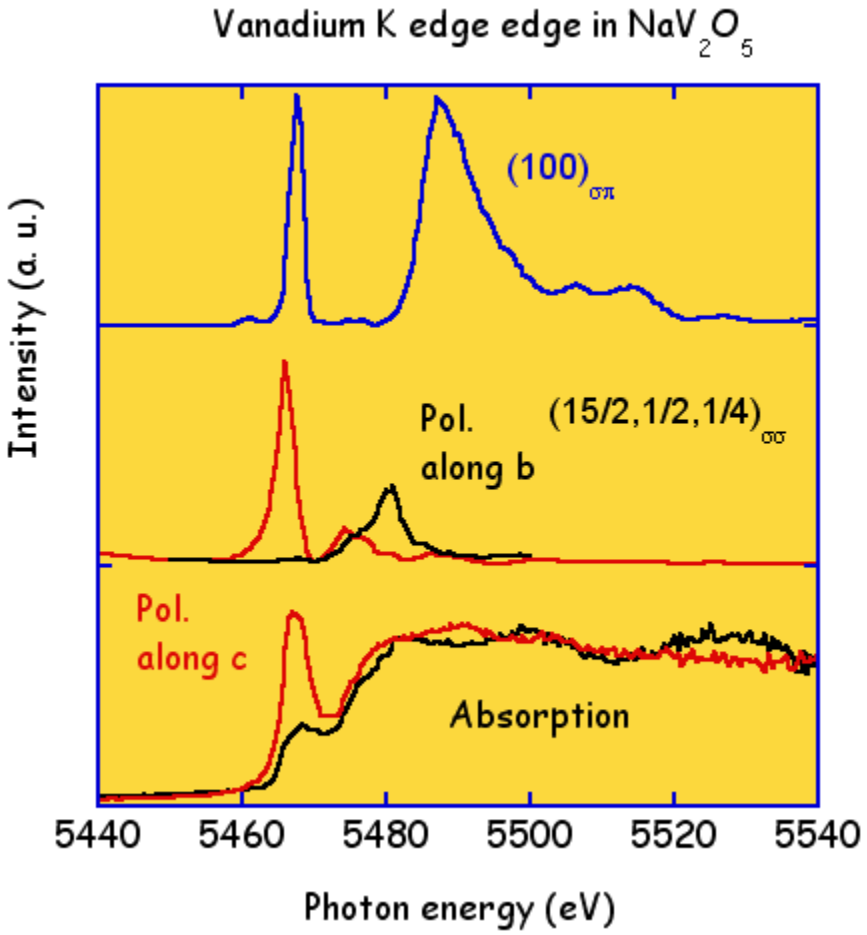

NaV_2O_5
S. Grenier *et al.*
ID20 /ESRF

Forbidden reflections visible just a the pre-edge

VOLUME 69, NUMBER 10 PHYSICAL REVIEW LETTERS 7 SEPTEMBER 1992

Resonant X-Ray Diffraction near the Iron *K* Edge in Hematite (α-Fe_2O_3)

K. D. Finkelstein, Qun Shen, and S. Shastri
Cornell High Energy Synchrotron Source (CHESS), Cornell University, Ithaca, New York 14853
(Received 7 May 1992)

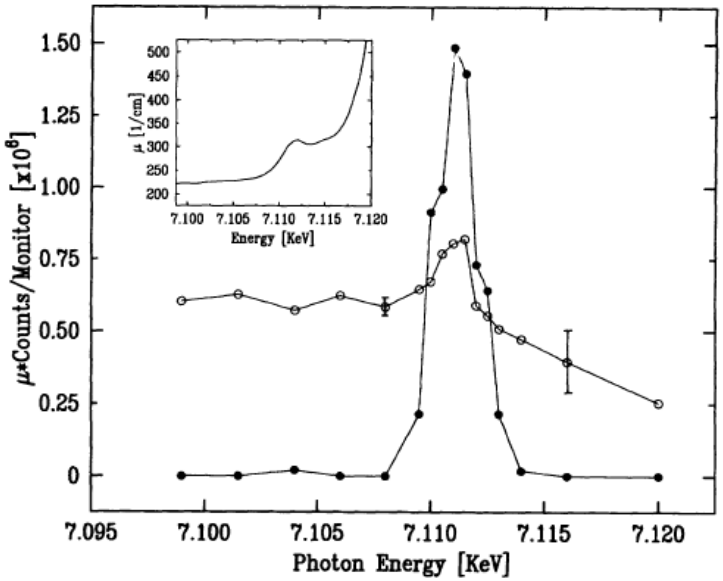

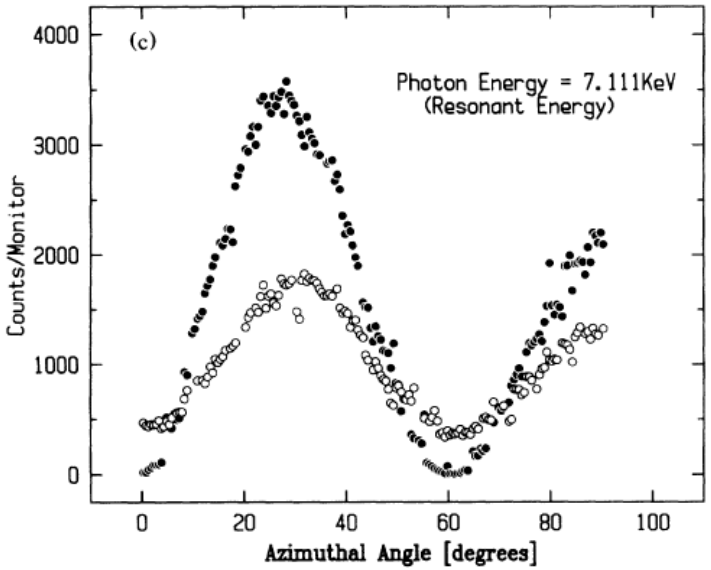

Forbidden Thomson and forbidden E1E1 (dipole-dipole)

Sensitivity on electronic properties ….

VOLUME 80, NUMBER 9 PHYSICAL REVIEW LETTERS 2 MARCH 1998

Direct Observation of Charge and Orbital Ordering in $La_{0.5}Sr_{1.5}MnO_4$

Y. Murakami,[1] H. Kawada,[1] H. Kawata,[1] M. Tanaka,[1] T. Arima,[2] Y. Moritomo,[3] and Y. Tokura[4,5]

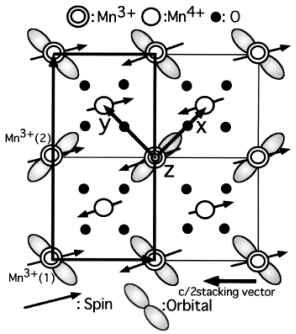

FIG. 1. Schematic view of the charge, spin, and orbital ordering in a layered perovskite manganite, $La_{0.5}Sr_{1.5}MnO_4$. The stacking vector along the c axis is shown in the figure.

$$F(h/2,h/2,0) \propto (f'^{3+} - f'^{4+}) + i(f''^{3+} - f''^{4+}) + C$$

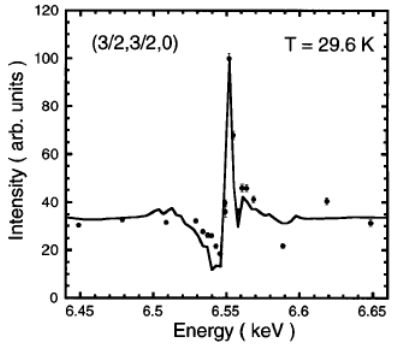

FIG. 2. Energy dependence of the charge-ordering superlattice reflection $(3/2, 3/2, 0)$ near the manganese K-absorption edge at $T = 29.6$ K. The solid curve is a calculated one based on $f'(E)$ and $f''(E)$ of Mn^{3+} and Mn^{4+}.

VOLUME 81, NUMBER 3 PHYSICAL REVIEW LETTERS 20 JULY 1998

Resonant X-Ray Scattering from Orbital Ordering in $LaMnO_3$

Y. Murakami,[1,2] J.P. Hill,[3] D. Gibbs,[3] M. Blume,[3] I. Koyama,[1] M. Tanaka,[1] H. Kawata,[1] T. Arima,[4] Y. Tokura,[5] K. Hirota,[2,6] and Y. Endoh[2,6]

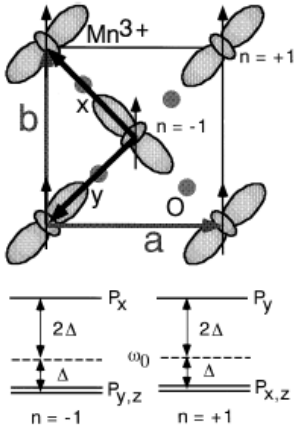

$$F = \sum_a e^{i\vec{Q}.\vec{R}_a} f_a = f_{Mn} - R_{90^\circ}(f_{Mn})$$

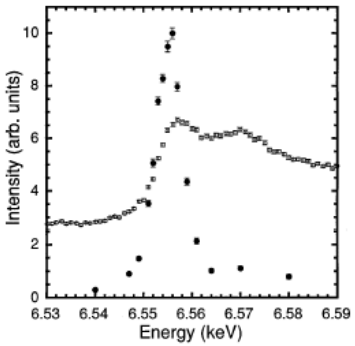

FIG. 2. Closed circles represent the energy dependence of the integrated intensity of the orbital ordering superlattice reflection $(3,0,0)$ with π' polarization near the manganese K absorption edge at $T = 10.0$ K. Open circles represent measured fluorescence. Similar results were obtained at the $(1,0,0)$ reflection.

Some materials has a transition resulting from a supposed charge disproportion between previously equivalent atoms

Does the charge ordering phenomenon exist ?

Is it possible to measure it with RXS ?

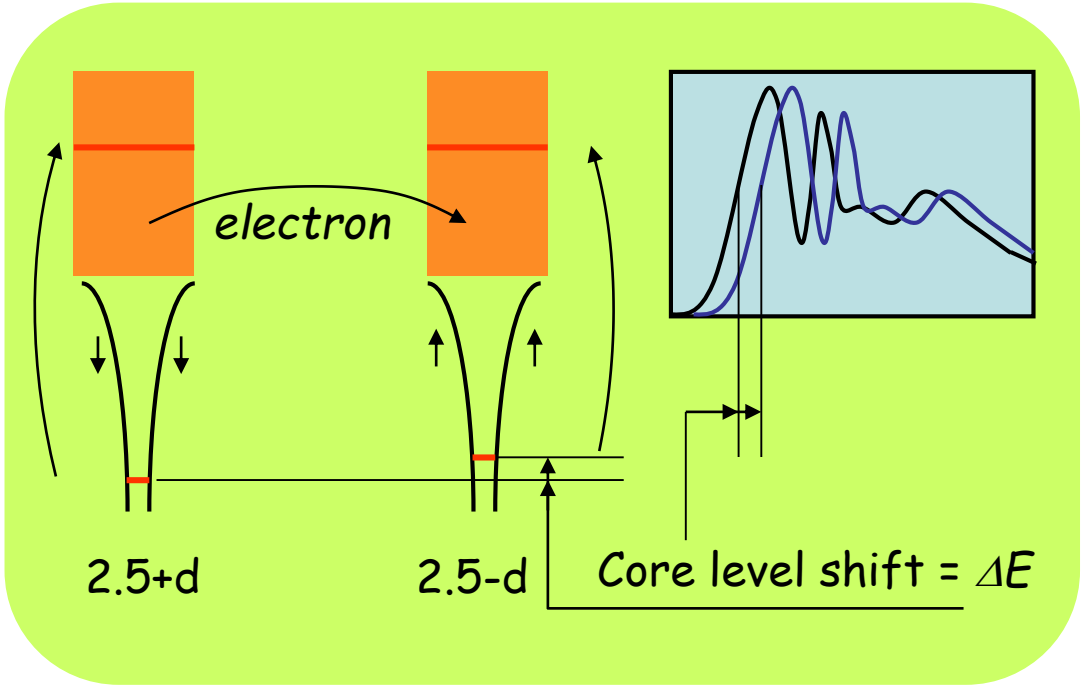

$$f^{2.5+\delta}(E) \approx f^{2.5}(E + \frac{\Delta E}{2})$$

$$f^{2.5+\delta} \approx f^{2.5} + \frac{\partial f^{2.5}}{\partial E}\frac{\Delta E}{2}$$

$$f^{2.5-\delta} \approx f^{2.5} - \frac{\partial f^{2.5}}{\partial E}\frac{\Delta E}{2}$$

$$F = f^{2.5+\delta} - f^{2.5-\delta} \approx \frac{\partial f^{2.5}}{\partial E}\Delta E$$

Study of charge ordering in magnetite in Cc

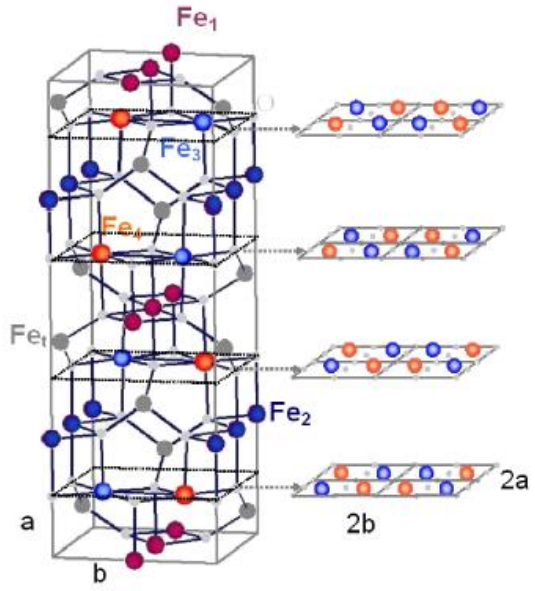

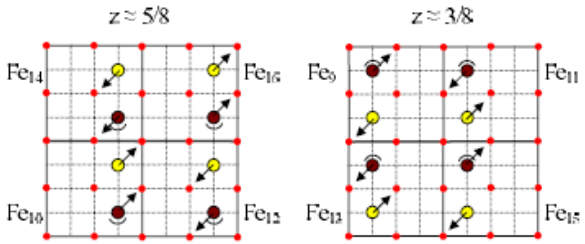

Experiment at Xmas (ESRF)

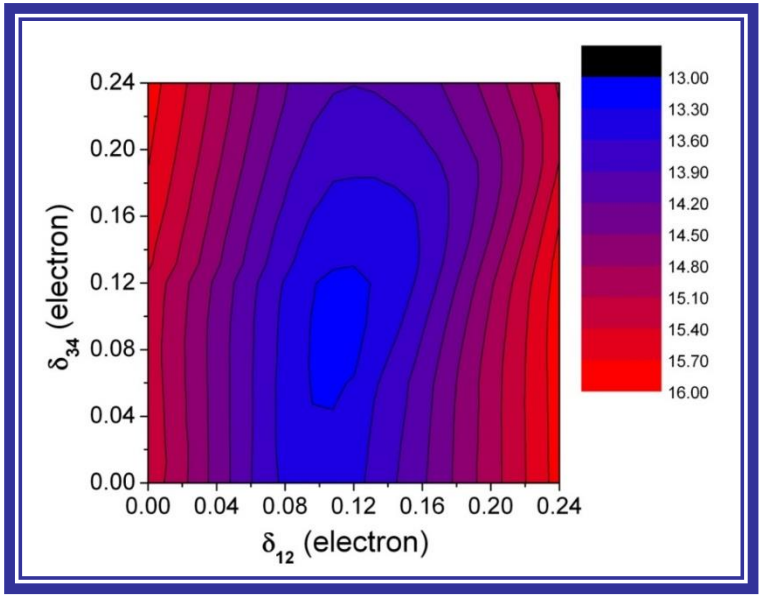

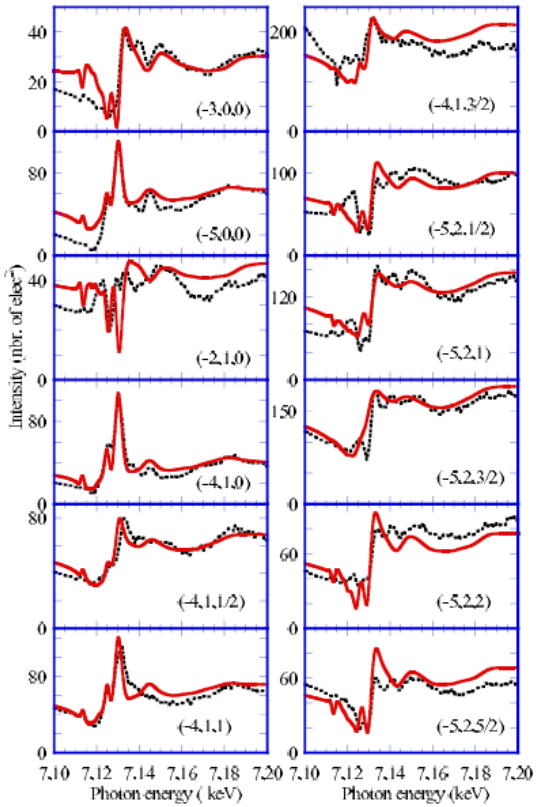

Fe_1-Fe_2 ± 0.12e-
Fe_3-Fe_4 ± 0.10e-

Cc index	δx	δy	δz	δcharge
9	0.0020	0.0015	0.000	0.025
10	0.0020	0.0015	0.000	0.050
11	−0.0020	−0.0015	0.000	−0.025
12	−0.0020	−0.0015	0.000	−0.050
13	0.0020	0.0015	0.000	0.000
14	−0.0020	−0.0015	0.000	0.025
15	−0.0020	−0.0015	0.000	0.000
16	0.0020	0.0015	0.000	−0.025

Elec. Pol. = 1.5 μC/cm² along *a*

XANES does not see anything !

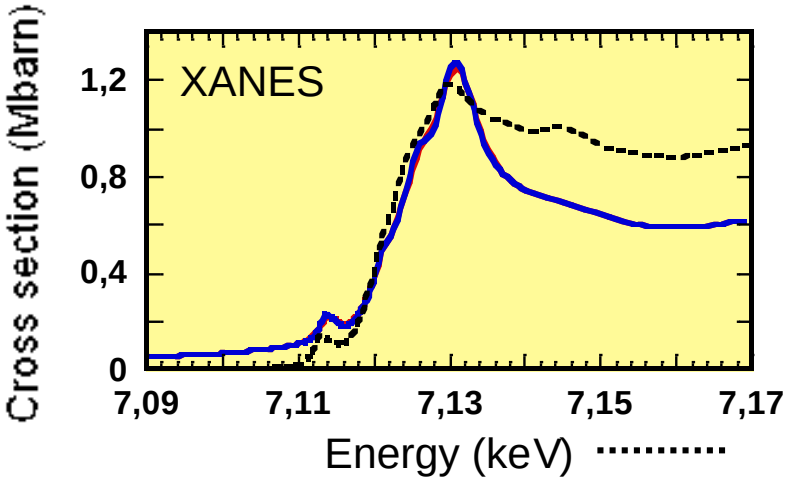

Surface resonant X-ray diffraction

Surface Resonant X-ray Diffraction (SRXRD)

$Au/Fe_3O_4/Ag(001)$

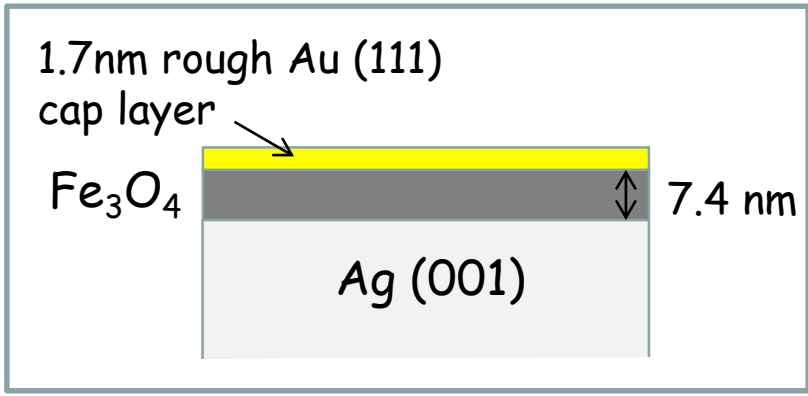

Entangled contributions of layer/substrate/cap layer

$$\left| F_{Fe3O4\ film}(Q,E) + F_{Ag}(Q) + F_{Cap\ layer}(Q) \right|^2$$

Specular crystal truncature rod

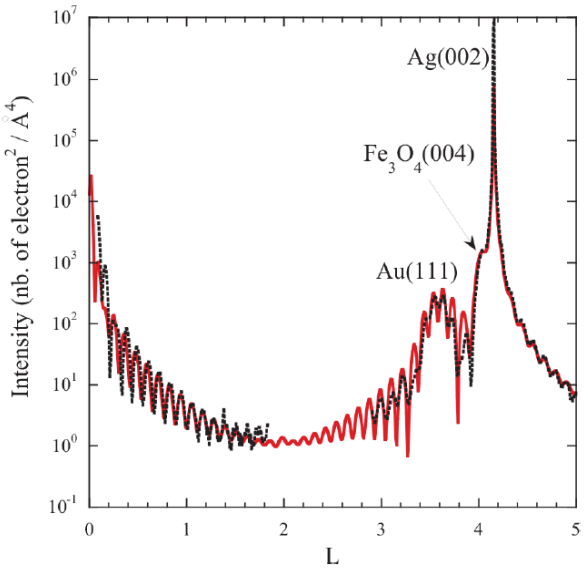

Spectra at L = 1.00

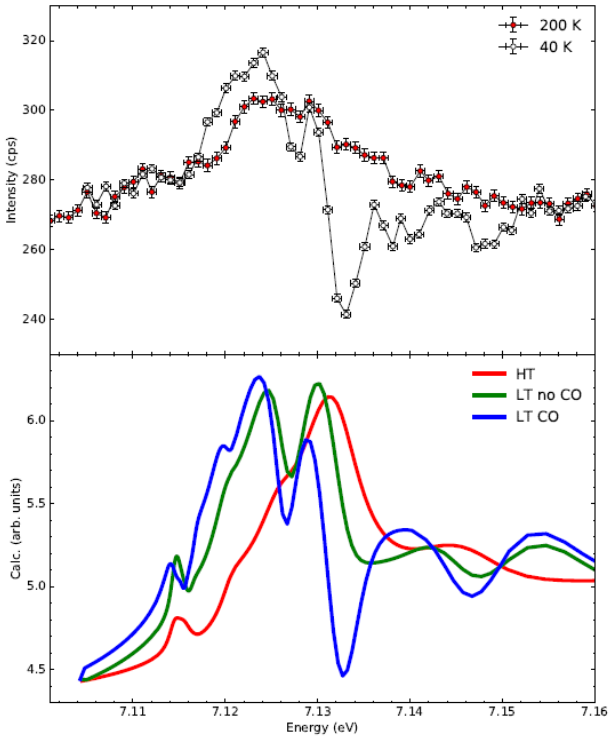

Verwey transition with charge ordering in a very thin Fe_3O_4 film !

S. Grenier *et al.* PRB 2017

Electrochemical interface: Br/Cu/Au(100)

With Yvonne Grunder, University of Liverpool

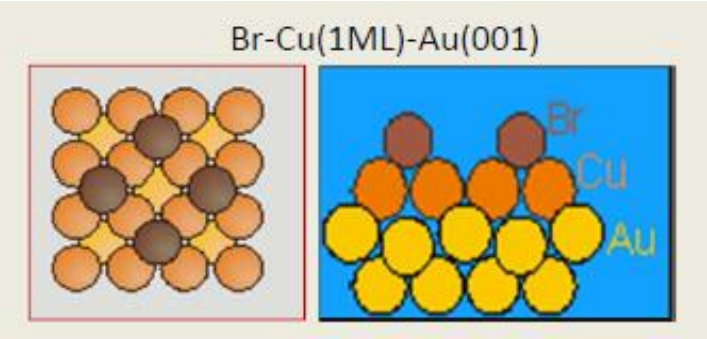

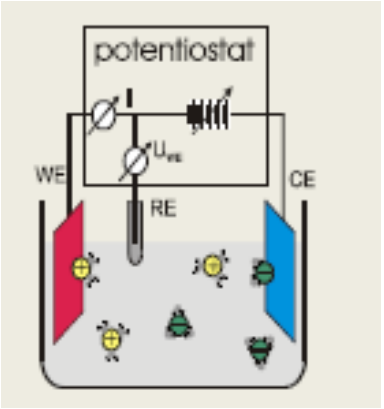

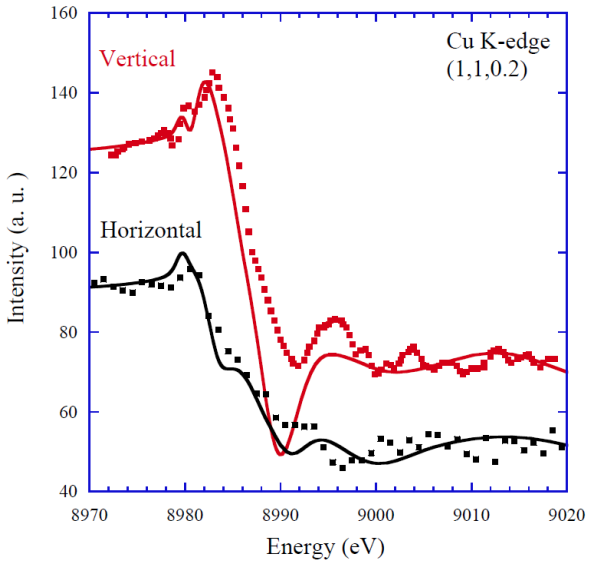

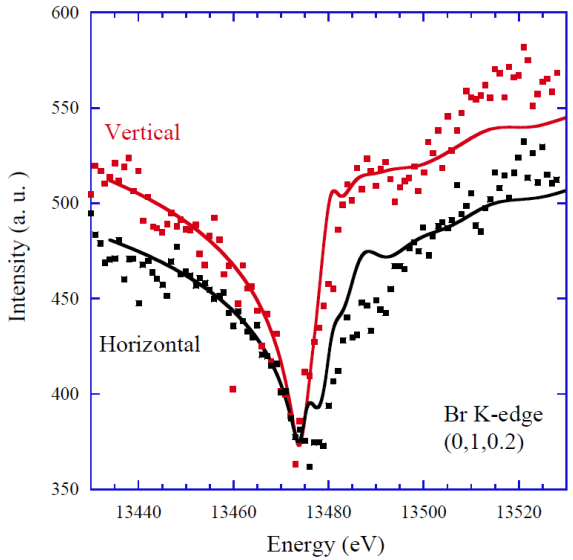

Dependence versus polarization

Exp: Xmas, ESRF

→ Sensitivity on bonding and oxidation state at the electrochemical interface

Y. Joly *et al.* JCTC 2018

Tutorial on FDMNES

The FDMNES code

1995: ESRF at Grenoble + Denis Raoux + Rino Natoli
→Starting of the XANES theoretical study

1996: first version of FDMNES
XANES calculation beyond the muffin-tin approximation
XAFS IX, Grenoble, August 26-30, 1996

1999: Resonant diffraction

2000–2009:
Multiple Scattering Theory
Magnetism - Spin-orbit
Space group symmetry analysis
Tensor analysis
Fit procedure
Self-consistency

2010-2018:
LDA + U, TD-DFT
XES (valence to core)
X-ray Raman
Surface resonant X-ray Diffraction

COOP

Input and output files

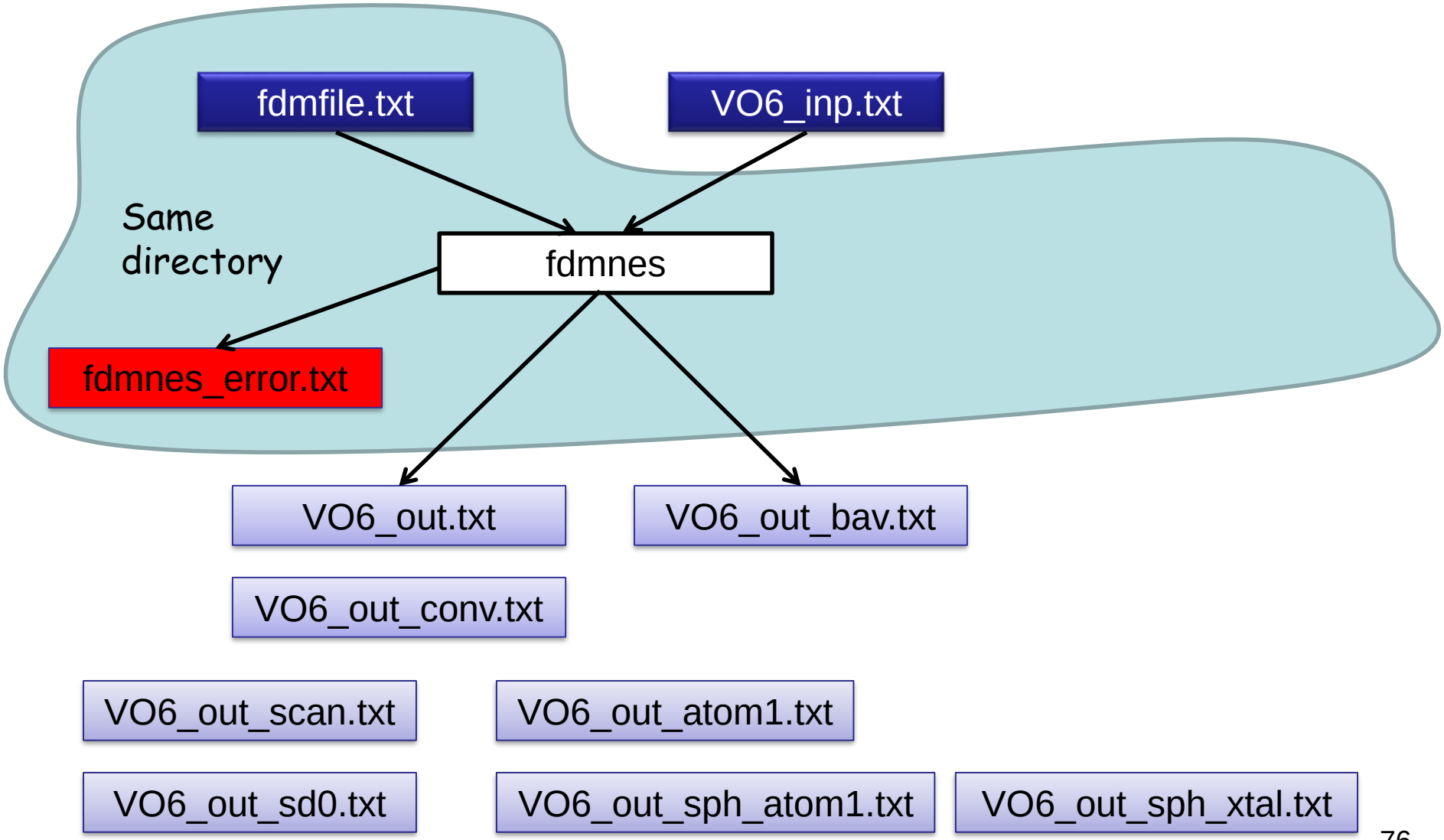

Examples of FDMNES indata file

```
Filout
  Sim/VO6

Range
 -2.   0.1   0.  0.5    60.

Radius
2.5

Quadrupole

Polarization

Molecule
 2.16  2.16  2.16  90. 90. 90.
 23  0.0   0.0   0.0
  8  1.0   0.0   0.0
  8 -1.0   0.0   0.0
  8  0.0   1.0   0.0
  8  0.0  -1.0   0.0
  8  0.0   0.0   1.0
  8  0.0   0.0  -1.0

Convolution

End
```

```
Filout
Sim/Fe3O4

Range
 -2. 0.1 -2.  0.5 20. 1. 100.

Radius
 5.0

Green
Quadrupole

DAFS
 0 0 2   1 1   45.
 0 0 6   1 1   45.
 4 4 4   1 1    0.


Spgroup
 Fd-3m:1

Crystal
       8.3940   8.3940   8.3940  90   90   90
 26    0.6250   0.6250   0.6250   ! Fe 16d
 26    0.0000   0.0000   0.0000   ! Fe  8a
  8    0.3800   0.3800   0.3800   ! O  32e

Convolution

End
```

Examples of FDMNES indata file

```
Filout
  Sim/VO6

Range
 -2.   0.1   0.  0.5    60.

Radius
2.5

Quadrupole

Polarization

Molecule
 2.16  2.16  2.16  90. 90. 90.
 23  0.0   0.0   0.0
  8  1.0   0.0   0.0
  8 -1.0   0.0   0.0
  8  0.0   1.0   0.0
  8  0.0  -1.0   0.0
  8  0.0   0.0   1.0
  8  0.0   0.0  -1.0

Convolution

End
```

```
Filout
Sim/Fe3O4

Range
 -2. 0.1 -2.  0.5 20. 1. 100.

Radius
 5.0

Green
Quadrupole

DAFS
 0 0 2   1 1   45.
 0 0 6   1 1   45.
 4 4 4   1 1    0.


Cif_file
Sim/in/Fe3O4.cif




Convolution

 End
```